KTH Information and Communication Technology

Digital Pre-compensation of Chromatic Dispersion in QPSK high speed telecom systems

MARIA SOL LIDON

Master of Science Thesis
Supervisor: Prof. Gunnar Jacobsen (ACREO AB)
Examiner: Assoc. Prof. Sergei Popov (KTH)

TRITA-ICT-EX-2011:209

Abstract

Chromatic dispersion (CD) is one of the most significant impairments in optical fiber communication systems. Since expensive and complex optical components are required to mitigate CD in the optical domain high-speed digital signal processing techniques are becoming an alternative to compensate electronically both non-linear and linear optical fiber degradations in the transmitter or receiver.

This thesis investigates a new electronic dispersion compensation technique based on signal predistortion using an electro-optic modulator driven by signals previously filtered by a linear Finite Impulse Response filter. Moreover, since transmitter and local oscillator lasers phase noise has usually been assessed independently without regard to the effect of chromatic dispersion on the phase noise in the system performance, a comparative study between pre- and post-compensation of chromatic dispersion influence on equalization enhanced phase noise (EEPN) in coherent multilevel systems is carried out. For that purpose, carrier phase estimation is implemented by a one-tap normalized least-mean-square filter.

Simulations of chromatic dispersion equalization in the transmitter demonstrate that a 56-Gbit/s QPSK coherent system is able to compensate large amounts of fiber chromatic dispersion using a predistorting linear finite impulse response filter. Concerning impact of chromatic dispersion compensation on equalization enhanced phase noise, simulation results show for post-compensation scheme the local oscillator phase noise limits the EEPN influence in the system. However, when the CD equalization is performed in the transmitter, the transmitter laser phase noise is the limiting factor that determines the EEPN effect in the transmission system. Most of those constraints may be mitigated by performing CD compensation in optical domain in such a way that the EEPN influence could be neglected.

Acknowledgements

First, I would like to thank my supervisor at KTH, Associate Prof. Sergei Popov, for his guidance, supporting me in my research and always being accessible when I have needed his help.
Specially I want to thank my supervisor at Acreo, Prof. Gunnar Jacobsen because of his huge work of support, guidance and the amount of time he devoted to the project. Also because he has shared his wide knowledge with me and for being very patient and encouraging me to solve all the obstacles that I got during my research work. Without him, I doubt this would have come to a good end.

I would like to thank Tianhua for his kind help in everything from the very beginning, always being accessible to all interesting discussion sessions during my thesis work.
I would like to also thank Mohsan Niaz for his endless help, his 'technical assistance', always being available for any discussion and being a huge font of knowledge. I will always be indebted to him.

Moreover, I want to thank all the people at Acreo, my partners and friends, specially Iñigo Sedano and Qu Shuai, although both of them left before I could finish this work I will always remember their kind help from my first day at Acreo, their hospitality and optimism. I learnt many things from them, I wish them all the best. And also Hou-Man, with whom I have spent so many good moments, thanks for cheering me up during discouraged times and being really nice company. I also want to thank Anna, Pontus, Viktor, Roland, Daniel for making me feel like if I was part of a small family at Acreo, being great friends always taking care of me and helping me with everything.

Thanks to all people that made me feel good during my stay in Stockholm, specially my 'Swedish' friends, Reyhaneh, Shabnam, Mozhgan for always being very close friends during my last year in Stockholm. I will never forget any of the great moments we spent together.

Furthermore, I want to thank my mother for her deep support during the degree and because without her help and love I would not be here. Thanks for encourage me during all my life and letting me decide in each moment what I wanted to do with my life. Also I want to thank my brother Julio for his guidance during all my life. Lastly, I especially would like to thank Jose for helping me become who I am today, encouraging me despite all the difficulties during last years, because we grew up together I have learnt many things from you that I will never forget. Thanks for making me believe in myself everyday.

Contents

List of Figures

Chapter 1

Introduction

The fast development of optical communication systems has revolutionized telecommunications technologies. Due to the high carrier frequency used to convey information in such systems which normally is roughly 200 THz, compared to microwave carrier frequencies in the GHz range, much higher transmission data rates (in the Terabit per second range) can be achieved in fiber-optic systems [1].

However, when trying to further increase the transmission rate in fiber-optic communication systems we are faced with multiple constraints, mainly due to impairments in the optical fiber such as chromatic dispersion, attenuation, and nonlinear effects. These constraints limit the available bandwidth in the fiber as well as the physical transmission range of the systems. For years these impairments have been dealt with in the optical domain through optical components such as Erbium Doped Fiber Amplifiers (EDFA) or Dispersion Compensating Fibers (DCF) which are used to compensate for the attenuation introduced by the fiber and to mitigate the chromatic dispersion effects. These methods however do have several drawbacks such as their high cost or potential loss in the quality or power of the signal.

In the recent years has increased the use of advanced digital signal processing (DSP) techniques in the electrical domain as an efficient and cost-effective alternative to optical domain compensation of fiber impairments , specially for impairments equalization in fiber-optic transmission systems. This is partly made possible by the availability of increasingly faster and cheaper digital signal processors. The development of high-speed digital electronics allows us, besides the compensation of optical degradations, also to achieve a higher spectral efficiency by using more advanced modulation formats, such as Quadrature Phase-Shift Keying (QPSK), which require coherent optical transmission systems [2].

Many different DSP methods have been developed for coherent optical communication systems in order to compensate for the fiber impairments at the receiver [3–5]. Furthermore, new DSP techniques are emerging to electronically mitigate fiber optical impairments not only at the receiver but also at the transmitter by predistorting the signal using an electro-optical modulator, for example a Mach-

Zehnder modulator is preferred for long-haul high-speed communication systems [6–10], which is driven by electrical predistorted signals. These DSP methods look very promising due to the fast progress of the industry in delivering both new faster sampling rate digital to analog converters (DACs) and higher capability Field-Programmable Gate Arrays (FPGAs) [11–13].

The main goal of this thesis is to design and analyze the performance of a linear finite impulse response filter for digital compensation of chromatic dispersion at the transmitter in a fiber-optic system. Moreover, it is carried out a careful study of the phase noise influence in a coherent transmission system with electronic dispersion equalization. Chapter 1 starts with an introduction to fiber-optical communication systems, presents some of the impairments that exists in such systems, as well as explains some solutions for counteracting the impairments besides stating main goal of this thesis.

In Chapter 2 a generic fiber-optic communication system is described. Its different components such as the electro-optic transmitter, the different modulation formats, the transmission link with its impairments, and the optical receiver are analyzed in detail.

Chapter 3 studies different techniques to perform electronic predistortion in the transmitter in order to compensate for the chromatic dispersion introduced by the fiber. Different transmitter modulation configurations are analyzed, first using an ideal amplitude/phase modulator in a cascade setup and later using a Cartesian Mach-Zehnder modulator. Here a linear finite impulse response filter is considered for equalization of the chromatic dispersion. This filter can be implemented both in the time and frequency domain, however, only time domain implementation is characterized in this thesis. Towards the end of this chapter simulation results of chromatic dispersion compensation are presented and analyzed.

In Chapter 4 different DSP algorithms for carrier phase estimation are investigated, in particular the Least Mean Square filter. Moreover, the influence of digital chromatic dispersion equalization (implemented at the transmitter and also at the receiver) on EEPN in a coherent multilevel system is assessed. At the end simulations results for post-compensation and pre-compensation schemes are reviewed and compared.
Finally, this thesis is ends with conclusions and future work in Chapter 5.

Chapter 2

Optical Fiber Communication Systems

2.1 Transmitter and modulation formats

The generic setup of a fiber-optic transmission system consists of a transmitter, where the data bits are modulated on a optical carrier using a specified modulation format, an optical fiber and an optical receiver, which reconstructs the transmitted signal. The transmitter has to convert the signal from the electrical domain to the optical domain before sending it through the optical fiber by using an electro-optical modulator. In the same way, the optical receiver is responsible for converting the optical signal back into the electrical domain.

2.1.1 Electro-optical modulators

Two methods are commonly used in order to perform the electro-optical conversion: direct and external modulation.

With direct modulation the output power of the light source (a light-emitting diode or a laser) is directly proportional to the electrical input signal. One of the main advantages of using direct modulation is that is cheap and simple to implement. It does however have some disadvantages, the switching of the input current causes a variation of the instantaneous frequency which leads to a chirp effect and the modulation speed is very low (normally not higher than 10 Gb/s). With external modulation an external device is responsible for modulating the intensity and/or phase of the optical source, the laser emits a continuous wave. External modulation is typically used in high-speed transmission systems such as long-haul telecommunication systems. The main advantages of such modulation is the high modulation speed achieved and less chirping effects than when using direct modulation [14].

Mach-Zehnder modulator configuration

One of the most common external modulators used is the Dual Drive Mach-Zehnder modulator (DDMZM) which is shown in figure 2.1. A DDMZM is a device composed

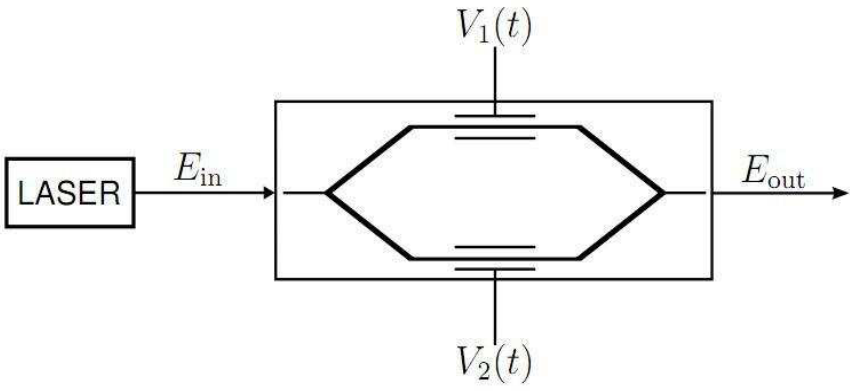

Figure 2.1: Dual drive Mach-Zehnder modulator [15].

of a divider, two optical fiber arms and a combiner. It is based on the wave interference phenomenon, the incoming optical signal is split into two signals, each one going through a different optical path, that then are recombined. The recombination produces constructive interference if the phase difference between the two signals is zero, if the phase difference between the combined signals is equal to π the signals will interfere destructively and the output light intensity will be near zero. The waveguides on each arm are made out of an electro-optical material, typically lithium niobate (LiNbO3), whose refractive index changes when a external voltage is applied to two electrodes placed on both sides of the waveguide. Changing the applied voltage causes phase shifts variations between the recombined signals and thus modulates the optical input signal.
The transfer function of a DDMZM is given by [16]:

$$\frac{E_{out}(t)}{E_{in}(t)} = \frac{1}{2}(e^{j\varphi_1(t)} + e^{j\varphi_2(t)}) \tag{2.1}$$

where $\varphi_1(t) = \pi\frac{V_1(t)}{V_\pi}$ and $\varphi_2(t) = \pi\frac{V_2(t)}{V_\pi}$ represents the phase shift in both arms of the Mach-Zender modulator (MZM).
Equation 2.1 can be written as follows [16]:

$$E_{out}(t) = E_{in}(t)\cos(\frac{\pi}{2}\cdot\frac{V_1(t) - V_2(t)}{V_\pi})e^{j\pi\frac{V_1(t)+V_2(t)}{2V_\pi}} \tag{2.2}$$

If the applied voltages are equal magnitude but with opposite sign, i.e. $V_2(t) = -V_1(t)$, $\varphi_2(t) = -\varphi_1(t)$ then the DDMZM acts as an amplitude modulator working in a *Push-Pull* configuration. Since the *chirp factor*, α, is proportional to phase variations in time, considering the phase term from equation 2.2, it is shown that for this configuration, the chirp factor is equal to zero, so *chirp-free* amplitude modulation can be achieved. In this case, from equation 2.2, the electric field at the output of the DDMZM will be expressed as:

$$E_{out}(t) = E_{in}(t)\cos(\frac{\pi V_1(t)}{V_\pi}) \tag{2.3}$$

On the other hand, if the applied voltages are equal, i.e. $V_2(t) = V_1(t) = V(t)$, $\varphi_2(t) = \varphi_1(t)$ then DDMZM is working in *Push-Push* mode. That means that the modulator is working as a pure phase modulator (no intensity modulation is performed). In this case the relationship between output and input electrical fields is given by:

$$E_{out}(t) = E_{in}(t)e^{j\frac{V(t)}{V_\pi}\pi} \tag{2.4}$$

The difference between the maximum and the minimum in the transfer function of the MZM is defined by V_π, which is one of the most important parameters to characterize these modulators.

Another significant issue is that the MZM must work in the linear zone of its transfer function, specifically in the Quadrature Point, QP which is placed in the middle of that linear zone. A correct voltage bias should be applied to achieve this QP.

In this thesis a Cartesian Mach-Zender modulator (figure 2.2) is used to generate a quadrature phase-shift keying modulation format (which has the same spectral efficiency as 4-QAM (Quadrature Amplitude Modulation)). A Cartesian MZM is composed of two Mach-Zehnder modulators, both in a *Push-pull* configuration, each one working as an amplitude modulator, which are used to modulate two signal components with a $\pi/2$ phase delay. As a result both the phase and intensity parameters can be controlled.

Although the dual drive Mach-Zender modulator has the advantages of lower cost, lower insertion loss, and simpler implementation, a Cartesian MZM is more appropriate when we are dealing with errors caused by digital signal processing limitations [11].

As seen above, it is possible to use Mach-Zehnder modulators to independently modulate intensity and phase of the optical field. However, there are other modulation setups that can be implemented in order to control multiple parameters

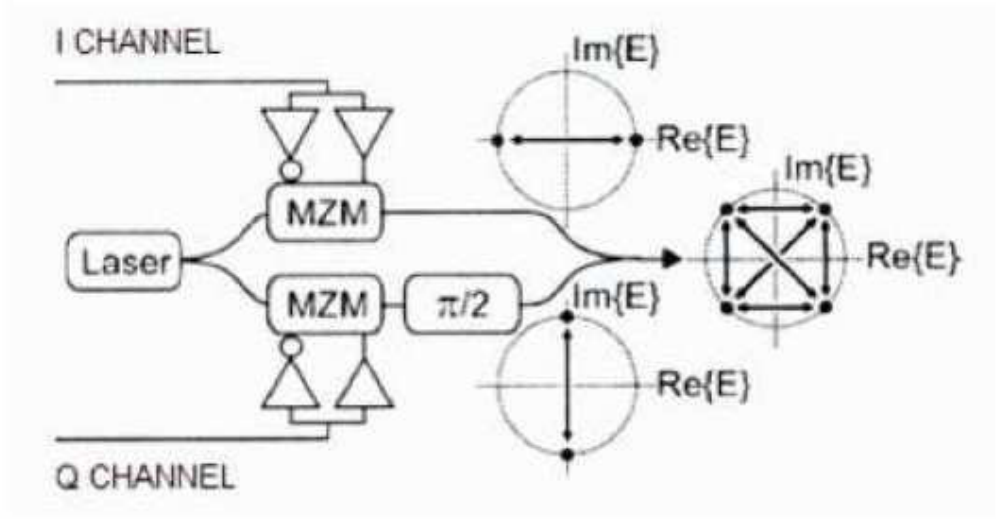

Figure 2.2: QPSK generation using Cartesian Mach-Zehnder modulator [17].

of the optical signal. One way to implement this is using a "serial configuration", such as an intensity modulator followed by a phase modulator, which gives control over multiple parameters of the optical carrier signal.

2.1.2 Modulation formats

In single mode fibers the optical field has four parameters that can be used to carry information: intensity, phase, frequency and polarization. Depending on which of the four parameters (or combinations of them) are used to convey the information, we distinguish between different modulation formats, such as Amplitude-Shift Keying, Frequency-Shift Keying, Phase-Shift Keying, Polarization-Shift Keying, and Quadrature Amplitude Modulation, a combination of Amplitude-Shift Keying and Phase-Shift Keying.

Amplitude-Shift Keying

Amplitude-Shift Keying is a digital modulation format based on amplitude variations of the optical carrier which are coded by different symbols. Each symbol consists of different number of bits depending on the number of modulation levels. For this kind of modulation phase, polarization, and frequency of the optical carrier is kept constant.

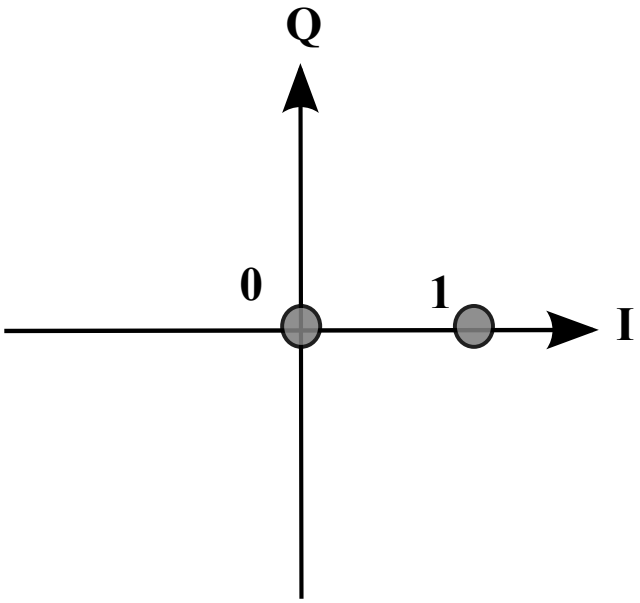

Figure 2.3: On-Off-Keying constellation diagram

On-Off Keying is the most common and simplest form of Amplitude-Shift Keying which only uses two different amplitudes. Each symbol is composed of one bit, absence of a carrier wave (no signal amplitude) denotes a '0' whereas bit '1' is denoted by existence of signal.

Regarding the spectral efficiency of the Amplitude-Shift Keying modulation format, the number of bits that can be conveyed in one symbol (η) can be defined as follows [18]:

$$\eta = \log_2 M[bps/Hz] \tag{2.5}$$

where M represents the number of modulation levels. For On-Off Keying, which only has two levels (on or off, M=2) the constellation diagram can be seen in figure 2.3.

Phase-Shift Keying

With Phase-Shift Keying (PSK) modulation the transmitted information is encoded in the carrier phase changes where each symbol has a specific phase. Two PSK formats are commonly used, Binary PSK (BPSK) and Quaternary PSK (QPSK or 4-PSK). In BPSK two symbols of one bit each are used as shown in figure 2.4, resulting in symbols with two phases with a phase difference of π radians. QPSK uses four modulation levels (four points in its constellation diagram distributed as shown in figure 2.5) with two bits per symbol. Therefore, the spectral efficiency of QPSK is double that of BPSK for a given bandwidth. In high data-rate systems with limited bandwidth BPSK is not suitable because of its low spectral efficiency of 1 [bps/Hz], and thus QPSK is only further considered.

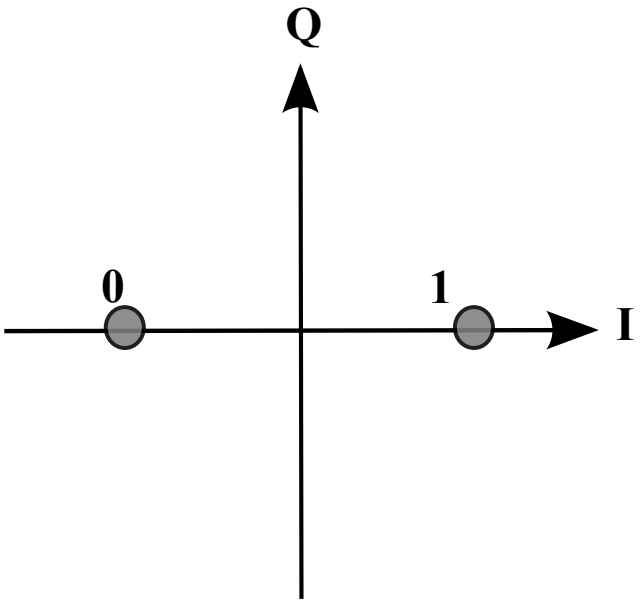

Figure 2.4: Binary PSK constellation diagram

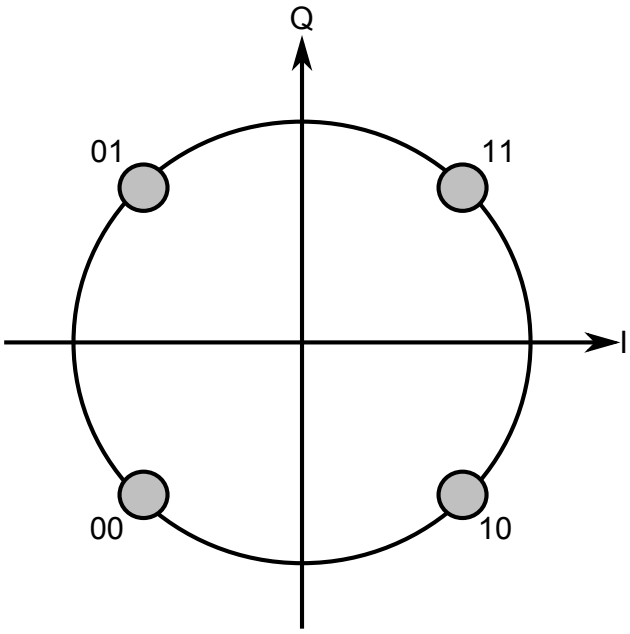

Figure 2.5: QPSK constellation diagram

While intensity and phase modulation formats have been widely used in high-speed optical communications, encoding information into the polarization of light (polarization shift keying, Pol-SK) has received less attention due to many factors as for example the additional receiver complexity needed for polarization management due to random polarization changes in optical fiber [19]. However, polarization is occasionally used in research experiments to increase the spectral efficiency by transmitting two different signals at the same wavelength but in two orthogonal polarizations (polarization-multiplexing) [20].

2.2 Transmission link

2.2.1 Propagation impairments in optical fibers

When the light propagates along a fiber it suffers some impairments which cause degradation of the original transmitted signal, these impairments can be divided into two classes, linear and non-linear.

For fiber-optic communication systems the propagation of one pulse through the optical fiber can be described by the non-linear Schrödinger equation [1]:

$$j\frac{\partial A}{\partial z} = \frac{\beta_2}{2}\frac{\partial^2 A}{\partial t^2} - j\frac{\alpha}{2}A - \gamma\left|A^2\right|A \tag{2.6}$$

where A is the electric field, β_2 is the dispersion parameter, α is the attenuation coefficient, and γ is the non-linear coefficient. Eq. 2.6 shows fiber impairments that lead to distortion in the transmitted signal.

Attenuation

The propagation of a pulse along a optical fiber produces power loss leading to a decrease of output power compared to the transmitted input power [16].

The variation of the average optical power P of a pulse propagating inside a fiber with respect to the fiber length L is described by the Beer's Law [1] as shown in equation 2.7:

$$\frac{\partial P}{\partial z} = -\alpha \cdot P \tag{2.7}$$

where α is the attenuation coefficient expressed in km^{-1} and z is the propagation direction. Thus the relationship between the input P_{in} and output power P_{out} of the fiber is:

$$P_{out} = P_{in} \cdot e^{-\alpha L} \tag{2.8}$$

Commonly the attenuation constant is measured in dB/km:

$$\alpha[dB/km] = \frac{-10 \cdot log(\frac{P_{out}}{in})}{L} \approx 4.343 \cdot \alpha \tag{2.9}$$

As can be seen in figure 2.6, the attenuation in a fiber depends on the wavelength of the transmitted light.

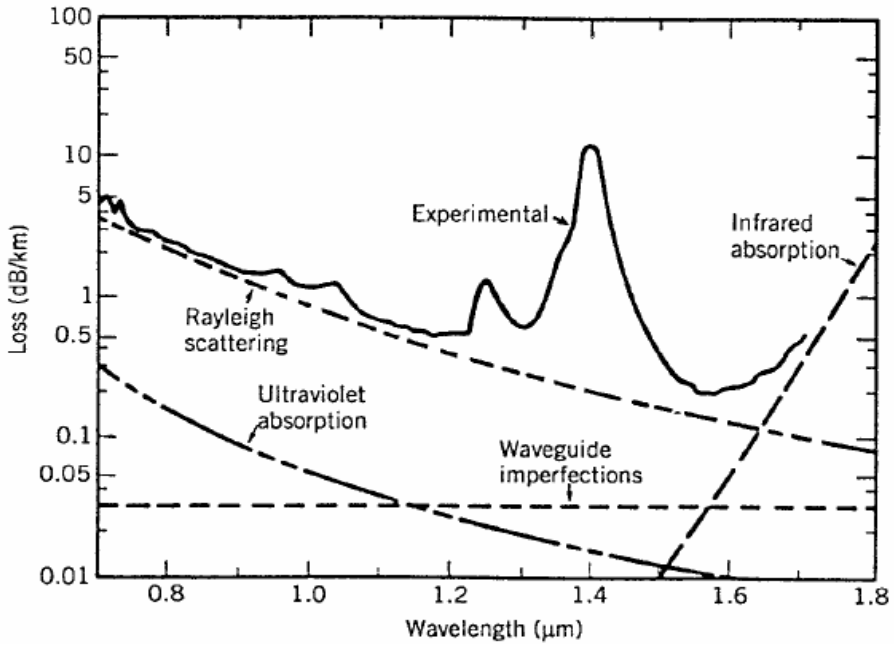

Figure 2.6: Optical fiber attenuation [1].

1. In the first window centered around $\lambda = 850\ nm$ the attenuation constant is $\alpha \approx 3 - 5\ dB/km$,

2. for the second window centered around $\lambda = 1330\ nm$ $\alpha \approx 0.5\ dB/km$,

3. for the third window centered around $\lambda = 1550\ nm$ the attenuation coefficient is $\alpha \approx 0.18\ dB/km$.

Since attenuation and dispersion effects are completely independent each other, they can be studied separately.

Chromatic Dispersion

One of the most significant linear impairments in fiber-optic communication systems is Chromatic Dispersion (CD). The light pulses that propagate along the optical fiber become distorted because different spectral components of the signal travel with different speed. This means that parts of the signal will reach the receiver at different time instants, resulting in a temporal pulse distortion. Dispersion causes a

reduction of the bandwidth since the pulse broadening limits the transmission rate. Dispersion is characterized by the parameter D, which describes how the pulse is widened. It increases with the transmission distance and also with the spectral linewidth of the optical source. In this thesis we will focus on long-haul fiber-optic transmission systems using a standard single mode fiber as the transmission link.

There are two physical issues accounting for the chromatic dispersion in optical fibers: One one hand, the *material dispersion* due to the fact that core and cladding are made of dispersive materials, meaning that the refractive index is frequency dependent, and the *waveguide dispersion* caused by the frequency dependence of the propagation constant along the waveguide.
Assuming that the fiber is a cylindrical dielectric waveguide along the z-axis, the wave propagation in the frequency domain along the positive z-coordinate is defined by [16]:

$$\underline{E}(z, j\omega) = \underline{E}(0, j\omega)exp(-j\beta(\omega)z) \tag{2.10}$$

where $\beta(\omega)$ is the frequency-dependent propagation constant. Making the Fourier series expansion around the carrier frequency $\omega_0 = 2\pi c/\lambda_0$ for pulses whose spectral width $\Delta\omega$ is much smaller than ω_0 [1]:

$$\beta(\omega) = \overline{n}(\omega)\frac{\omega}{c} \approx \beta_0 + \beta_1(\Delta\omega) + \frac{\beta_2}{2}(\Delta\omega)^2 + \frac{\beta_3}{6}(\Delta\omega)^3 + \dots \tag{2.11}$$

where $\Delta\omega = \omega - \omega_0$ and the series coefficients are written as:

$$\beta_n = (\frac{\partial^n \beta}{\partial \omega^n})_{\omega=\omega_0} \tag{2.12}$$

The group delay τ per unit of length is:

$$\frac{\tau(\omega)}{L} = \frac{\partial \beta}{\partial \omega} \tag{2.13}$$

The first term of Equation 2.11 represents a frequency independent phase rotation that can be disregarded for the propagation of the pulse. The second coefficient, $\beta_1 = \frac{1}{\nu_g}$, is equal to the group delay per unit of length and also equal to the inverse of the group velocity $\nu_g = n_g/c$ (ideal case, constant group delay). The third term of 2.11 describes first-order chromatic dispersion, also called group-velocity dispersion. The parameter $\beta_2 = \frac{d\tau}{d\omega}$ is the chromatic dispersion parameter and it is responsible for linear variation of group delay with frequency. Commonly chromatic dispersion parameter is written in terms of $\Delta\lambda$ instead of $\Delta\omega$:

$$D = \frac{d\tau}{d\lambda} = -\frac{2\pi c}{\lambda_0^2}\beta_2 \tag{2.14}$$

where the units of D are usually expressed as $ps/nm/km$. Typical values in standard single mode fiber the wavelength $\lambda_0 = 1550\, nm$ (third window) is: $\beta_2 = -21\, ps^2/km$

and $D = 17\ ps/nm/km$. As previously mentioned, the total dispersion parameter is given by the sum of both the material and waveguide dispersion as it is depicted in figure 2.7:

$$D_{tot} = D_m + D_{wg} \tag{2.15}$$

In standard single mode fiber the minimum attenuation is at a wavelength of 1550 nm, however, the dispersion parameter is not at a minimum in that window. One solution for this issue is to design *dispersion-shifted-fibers* in which it is possible to vary the waveguide dispersion parameter D_{wg} by modifying the structure of the fiber in order to get a total dispersion parameter equal to zero for third window.

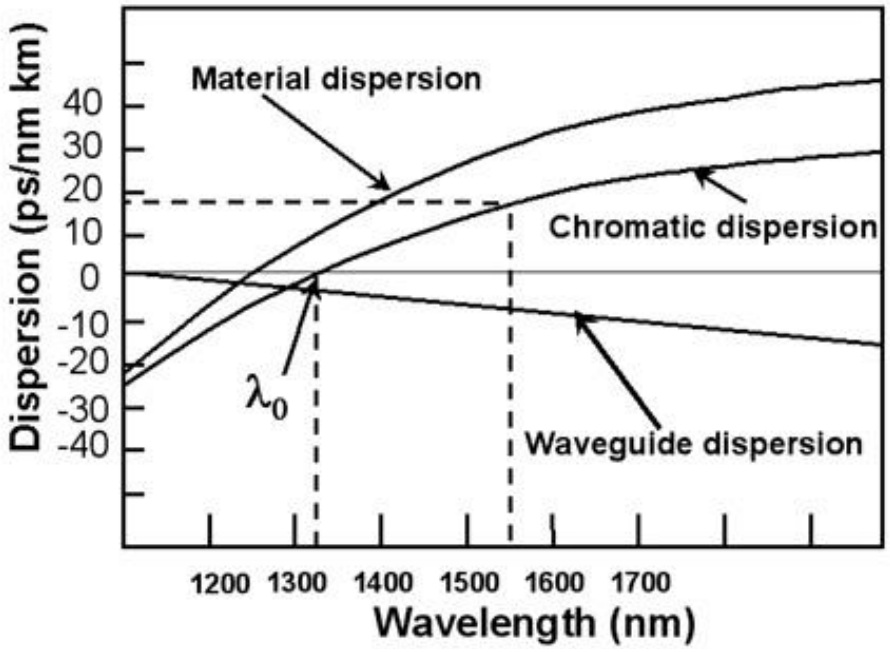

Figure 2.7: Total dispersion D_{tot} and relative contributions of material dispersion D_m and waveguide dispersion D_{wg} for a conventional single-mode fiber [1].

The fourth term in Equation 2.11 is related to the dispersion slope S. The dispersion slope can also be expressed in terms of wavelength using:

$$S = \frac{dD}{d\lambda} = (\frac{2\pi c}{\lambda_0^2})^2 \beta_3 \tag{2.16}$$

where the slope parameter S is generally expressed in units $ps/nm^2/km$. A typical value in standard single mode fiber for $\lambda_0 = 1550\ nm$ is $S = 0.08\ ps/nm^2/km$.

For a better understanding of the chromatic dispersion effect in the time domain we can study the propagation model of Gaussian pulses inside the optical fiber, specifically a single chirped Gaussian pulse. The initial field of the pulse is written as:

$$\underline{A}(0,t) = A_0 \exp(-\frac{1+iC}{2}(\frac{t}{T_0})^2) \tag{2.17}$$

where A_0 is the peak amplitude, C represents chirp parameter and T_0 is the half-width at $1/e$ intensity point. It is related to the full-width at half-maximum (FWHM) of the pulse by:

$$T_{FWHM} = 2(ln2)^{1/2} T_0 \tag{2.18}$$

As shown in [1], during its propagation along the fiber the Gaussian pulse keeps its Gaussian shape, however the pulse width increases with the propagation distance z resulting in a broadening factor given by:

$$\frac{T_1}{T_0} = \sqrt{(1-\frac{Cz}{L_D})^2 + (\frac{z}{L_D})^2}, \tag{2.19}$$

where T_1 represent the half-width defined similar to T_0 and $L_D = \frac{T_0^2}{|\beta_2|}$ is the *dispersion length.* For an unchirped Gaussian pulse (C=0), whose broadening factor is $\sqrt{1+(\frac{z}{L_D})^2}$, the dispersion length (L_D) is the distance after which a pulse is broadened by a factor $\sqrt{2}$. Hence this parameter is the relationship between a pulse parameter (T_0) and a fiber parameter (β_2). Otherwise for chirped pulses factor $\beta_2 C$ has an critical influence on the broadening or compression of the pulse. That means that for $\beta_2 C$ higher than zero the chirped Gaussian pulse broadens faster than a unchirped pulse whereas for $\beta_2 C$ lower than zero the pulse width initially decreases [16].

Pulse broadening caused by chromatic dispersion leads to intersymbol interference since when one symbol is broadened it interferes with the subsequent symbols. If dispersion compensation techniques are not used in the system, the transmission distance will be limited by this phenomenon.

Polarization mode dispersion

Standard single-mode fiber carries one fundamental mode, which consists of two orthogonal polarizations. Ideally the core of an optical fiber is perfectly circular and thus has the same refraction index for both polarization states. However, in a real fiber, mechanical and thermal stresses introduced during manufacturing result in asymmetries in the fiber core geometry which causes a birefringence phenomenon, which means that there is a different refractive index for each polarization state. The difference in refractive index causes the two polarization modes to propagate with different speeds. This phenomenon is called *Polarization Mode Dispersion* (PMD).

At the receiver the difference in propagation time between the two orthogonal polarizations of the pulse is called the *Differential Group Delay* (DGD), which causes a broadening of the input pulse (fig. 2.8).

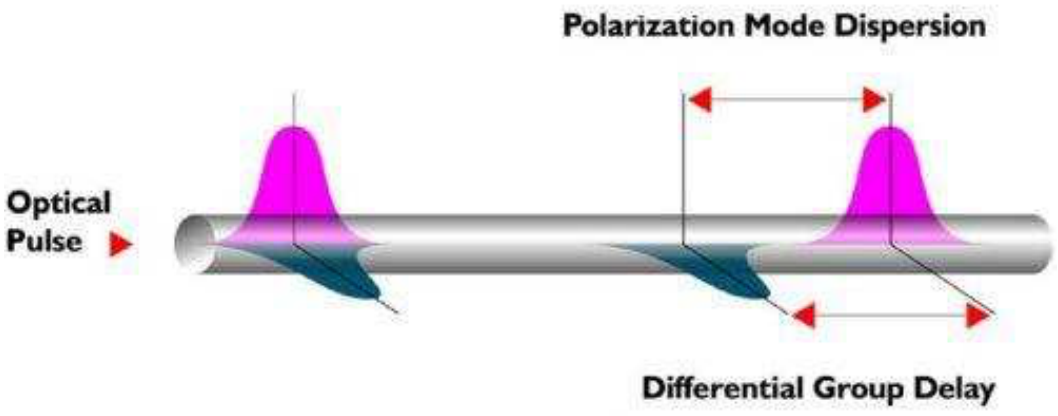

Figure 2.8: Impact of PMD on the propagating pulse .

For a fiber of length z, the total DGD can be calculated as:

$$\sigma(z) = D_p\sqrt{z} \tag{2.20}$$

where D_p is the PMD parameter, typically its value is about $0.1 - 1\ ps/\sqrt{km}$. The PMD effect can be compensated using digital signal processing in digital coherent receivers.

Nonlinear effects

Optical communication systems only experience linear effects as long as the launched level power is moderate, in the mili-Watt range. However, increasing the launched power of an optical signal the field intensity in the fiber is also increased which leads to nonlinear effects in the fiber. Nonlinearities can be classified in two categories:

The first category is power and intensity-dependent refractive index which is also known as the optical *Kerr effect*: self-phase modulation (SPM), cross-phase modulation (XPM), and four-wave mixing (FWM). The other category is nonlinear scattering effects: stimulated Raman scattering (SRS) and stimulated Brillouin scattering (SBS) [1].
From the Schrödinger equation in absence of dispersion setting $\beta_2 = 0$ we get:

$$A(t,z) = A(t,0)\exp(j\theta_{NL}(t,z)) \tag{2.21}$$

where $\theta_{NL}(t,z)$ represents the nonlinear phase shift given by:

$$\theta_{NL}(t,z) = \gamma P_0 \left|A(t,0)\right|^2 L_{eff} \tag{2.22}$$

$$L_{eff} = 1 - \exp(-\alpha z)/\alpha \tag{2.23}$$

where P_0 is the peak power of the pulse and α represents fiber losses. From equation 2.22 it can be seen that the nonlinear phase shift is proportional to the pulse intensity, in such a way that different pulse components suffer different phase shifts leading to an optical pulse with a certain chirp which will modify pulse dispersion effects. This phenomenon is called self-phase modulation (SPM). The SPM-induced chirp impacts the pulse shape through group-velocity dispersion and it causes additional pulse broadening.

In addition, a significant limitation of optical systems performance is the spectral broadening of the pulse produced by SPM which increases the signal bandwidth substantially. Furthermore, in high bit rate Wavelength Division Multiplexing (WDM) systems, where different wavelengths are multiplexed and transmitted through the same optical fiber, it is important to classify the nonlinear effects into *intrachannel* and *interchannel* non-linearity's.

Intrachannel non-linearity's characterize the nonlinear effects in a single wavelength channel whereas interchannel non-linearity's concern the non-linear effects between neighboring wavelength channels. WDM systems are highly affected by interchannel effects such as cross-phase modulation (XPM) in which one wavelength produces phase shifts of another wavelengths and four-wave mixing (FWM) where three different wavelengths interact to create a new wavelength. Furthermore, the FWM effect becomes more critical in optical systems where the dispersion is compensated and where there is a low distance between different frequencies.

2.3 Coherent Optical Receiver

In the optical receiver the signal is converted from the optical to electrical domain by photodetectors placed in the receiver. When using only a photodetector that operates as an intensity envelope detector it is called Direct Detection. However, using this detector the phase information of the optical signal is lost, thus Direct Detection is not used in coherent receivers. Since we want to use multilevel modulation formats, such as M-PSK, M-QAM in order to improve the spectral efficiency, coherent detection is required.

In a coherent detector the receiver recovers the full electric field containing both amplitude and phase information. Information can be encoded in amplitude and phase, or alternatively in both the in-phase and the quadrature components of a carrier. Coherent detection requires the receiver to have knowledge of the carrier phase, as the received signal is demodulated by a local oscillator that acts as a phase reference.

In a coherent detection receiver, such as that is shown in Figure 2.9, the incoming signal is mixed with the four quadratural states associated with the reference signal (the local optical oscillator) in the complex-field space. In this thesis that function is implemented by a 90 degrees optical hybrid, which is used for coherent signal

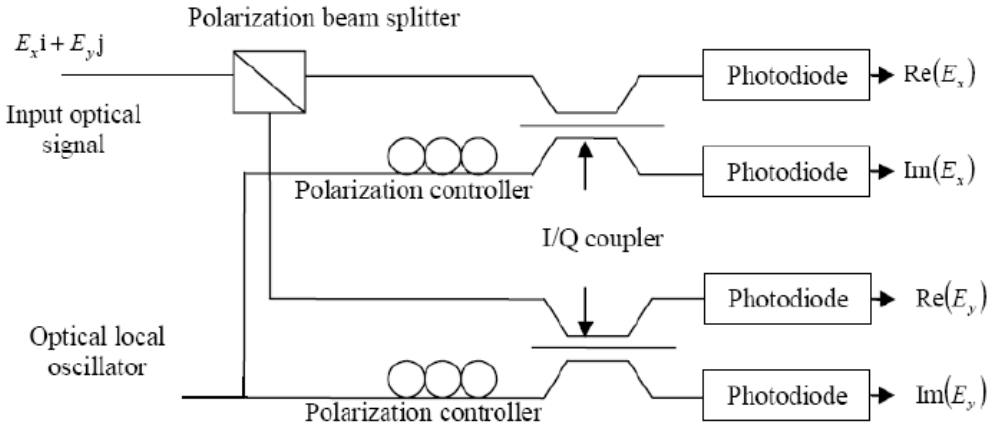

Figure 2.9: Schematic of a coherent receiver [21].

demodulation. After demodulation the optical hybrid conveys the four light signals to two pairs of balanced detectors.

The conversion from optical passband to electrical baseband can be achieved in a homodyne receiver, where the frequency of the local oscillator laser is adjusted to that of the transmitter laser so the photoreceiver output is at baseband. Then the electrical baseband signals obtained are sampled at Nyquist rate and digital signal processing can be applied to them in order to compensate fiber transmission impairments.

Chapter 3

Chromatic Dispersion Compensation by Signal Predistortion

Chromatic dispersion in the fiber can be compensated in both the optical and electrical domain. To perform chromatic dispersion compensation in the optical domain typically Dispersion Compensating Fibers (DCFs) are used in the transmission link in order to cancel out the accumulated dispersion. However, these modules have some drawbacks e.g. they increase the loss and attenuation and in that way reduce the system performance. They also have high non-linear distortion effects which further increases the cost of the final system.

On the other hand, interest is increasing for electronic compensation of chromatic dispersion using digital signal processing. Since chromatic dispersion is a linear phenomenon, the compensation can be placed either at the receiver or at the transmitter side. When the compensation is performed at the transmitter it is called precompensation, otherwise it is called postcompensation.

While most of the digital signal processing-based electrical chromatic dispersion compensation techniques have been implemented at the receiver, it has recently been shown that large quantities of CD can be entirely compensated using a transmitter based on electronic predistortion [6]. Consequently, it has recently become an attractive alternative to postcompensation.

3.1 Electronic predistortion transmitter

The main function of an electronic predistorted transmitter is to produce predistorted signals that, when being transmitted through a fiber, the fiber dispersion inverts the distortion added by the transmitter resulting in a clean signal waveform at the receiver.

As was mentioned in chapter 2, different transmitter modulator schemes can be used to perform the predistortion, in this thesis both configurations mentioned earlier, i.e. the serial AM/PM modulator and the Cartesian Mach-Zehnder modulator, are assessed.

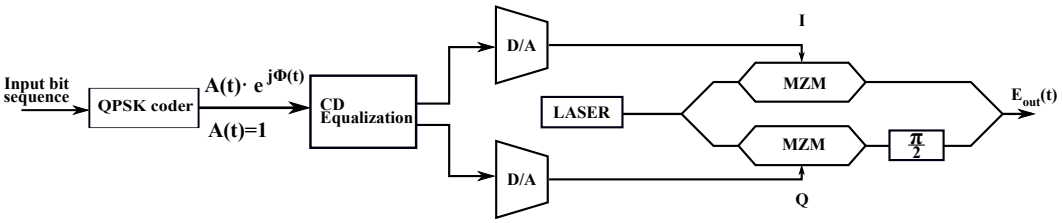

Figure 3.1: Transmitter configuration using Cartesian Mach-Zehnder modulator [8].

3.1.1 Using the Cartesian Mach-Zehnder Modulator

In a system using the Cartesian MZM the input bit stream is digitally filtered and converted into two analog signals by a digital-to-analog converter (DAC) before being used as the electrical inputs of the Cartesian Mach-Zehnder modulator (shown in figure 3.1). Either linear or nonlinear digital filtering can be used, however this thesis is focused on the performance using a linear finite impulse response filter.

In this transmitter setup predistorted signals are generated using a Cartesian MZM driven by voltages d_1 and d_2. As previously shown in section 2.1.1, the modulator output is supposed to be [12]:

$$E_{out} = \frac{E_{in}}{2}[\cos(\frac{\pi d_1}{V_\pi}) - i\cos(\frac{\pi d_2}{V_\pi})] \tag{3.1}$$

where E_{in} is the electric field input from a constant continuous wave laser, d_1 and d_2 are the drive signals for the MZM, and V_π is the voltage required to achieve a phase shift of π radians.

3.1.2 Using AM/PM Modulators in Serial Configuration

Serial (cascade) configuration, i.e. an amplitude modulator (AM) followed by a phase modulator (PM), is appropriate when we want to separately control different parameters in the modulation scheme.

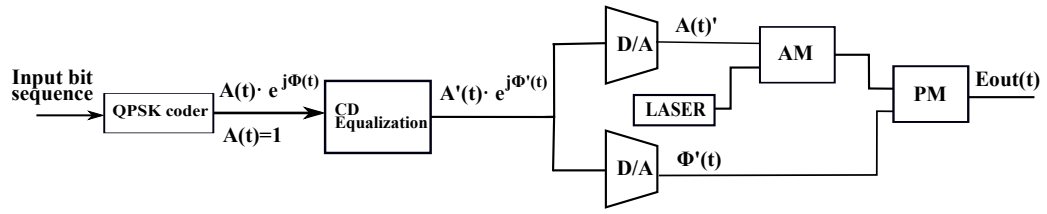

Figure 3.2: Transmitter for QPSK system with pre-compensation of chromatic dispersion. The QPSK modulation is indicated in the time domain by $A(t)exp(j\varphi(t))$ and the CD equalized signal by $A'(t)exp(j\varphi'(t))$. Figure abbreviations: D/A - digital to analogue conversion; CD - chromatic dispersion.

As it is depicted in figure 3.2 the digital sequence is filtered by a linear FIR filter and then converted to the analog domain. The two continuous signals, which carry the phase and amplitude information of the filter output signal, will be the drive signals for the PM and AM ideal modulators respectively. As seen in Figure 3.2 the modulators are placed in a cascade configuration. If the output signal of the amplitude modulator is written as:

$$\underline{E}_{out_{AM}}(t) = \underline{E}_{in}(t) * \sqrt{data_{A'}(t)} \tag{3.2}$$

where $\underline{E}_{in}(t)$ is the input optical signal, and $data_{A'}(t)$ the electrical modulation signal, then the output signal of the phase modulator is assumed to be:

$$\underline{E}_{out}(t) = \underline{E}_{out_{AM}}(t) * \exp(j \cdot \Delta\varphi \cdot data_{\varphi'}(t)) \tag{3.3}$$

where $\Delta\varphi$ is the phase deviation and $data_{\varphi'}(t)$ is the phase information electrical signal.
It is important to note that for serial configuration the output of the CD equalization module is split into two signals, amplitude and phase, which will control the amplitude and phase modulators. In the case of the MZM configuration, shown in figure 3.1, the drive signals are obtained by splitting the output of the CD compensation filter into its in-phase and quadrature signals.

In the serial configuration the modulation index for the AM modulator was set equal to 1 whereas in the PM modulator the phase deviation factor depends on the maximum phase at the output of the FIR filter which is closely related to the fiber length.

In the MZM setup the bias voltage is selected so that the MZM is working in the linear zone of its transfer function. Experimentally it was found that $V_{bias} = V_\pi/4$ is good to get good performance of the MZM, where $V_\pi = 3$ V.

Regardless of the configuration used, assuming the transmitted signal is altered by the accumulated dispersion of the transmission link, $\beta_2 * L$, where β_2 is the fiber dispersion constant, L is the fiber length, and the optical spectrum of predistorted transmitted signal $E_{tx}(\omega)$, the spectrum of the desired received signal can be stated as:

$$E_{rx}(\omega) = E_{tx}(\omega)\exp(-j\beta_2\omega^2 L/2) \tag{3.4}$$

3.2 Finite impulse response predistorting filter

There are several different digital signal processing methods that may be used to compensate the chromatic dispersion by electronic predistortion at the transmitter, for example applying non-linear filtering using Look-Up Tables (LUT) and linear FIR filtering. One of the main advantages in optical communications systems to perform signals predistortion is that only linear filtering is needed to counteract linear fiber impairments such as chromatic dispersion. However, nonlinear filtering

can be required to compensate fiber intra channel nonlinearities [11]. Since this thesis is focusing on chromatic dispersion compensation, FIR filtering has been employed.

3.2.1 Study of dispersion compensating filters

Before studying the design of dispersion compensating filters, we consider the physics behind the phenomenon of chromatic dispersion. As a continuation of what was described in section 2.2.1, the equation 3.5 characterizes the electro-magnetic wave propagation as shown previously. Moreover, it is interesting to study carefully the effect of the chromatic dispersion on the envelope $A(z,t)$ of a pulse. The electric field can be specified in terms of the varying pulse amplitude $A(z,t)$ by [1]:

$$E(z,t) = A(z,t)\exp(-j\beta_0 z + j\omega_0 t) \tag{3.5}$$

Considering a delay in the time axis, $t' = t - \tau z$ and the group velocity $\nu_g = 1/\tau$. Taking the Fourier transform of the varying envelope for $t = t' + \tau z$:

$$\underline{A}(z, j(\Delta\omega)) = \int A(z, t' + \tau z)\exp[-j(\Delta\omega)t']dt' \tag{3.6}$$

Taking into account equation 2.10, 2.11 and 2.12 the variation of the envelope in frequency domain can be described by:

$$\underline{A}(z, j(\Delta\omega)) = A(0, j(\Delta\omega))\exp(-j\frac{\beta_2}{2}(\Delta\omega)^2 z - j\frac{\beta_3}{6}(\Delta\omega)^3 z) \tag{3.7}$$

This means that each spectral component of the signal envelope gets a phase shift depending on frequency and propagation distance z. Finally, $A(z,t')$ can be estimated by taking the inverse Fourier transform of 3.7, which describes the time domain pulse envelope. In the absence of fiber nonlinearities and considering only β_2 (setting $\beta_3 = 0$), the partial differential equation for the pulse propagation in the time domain is derived obtaining $A(z,t')$ and differentiating it with respect to z.

$$\frac{\partial A(z,t')}{\partial z} = j\frac{\beta_2}{2}\frac{\partial^2 A(z,t')}{\partial t'^2} \tag{3.8}$$

where $j = \sqrt{-1}$, z is the propagation distance, λ is the wavelength of the light, c is the speed of light, and D is the dispersion coefficient of the fiber. From Eq. 3.7 we can deduce the frequency domain linear transfer function $\underline{H}(z, j\Delta\omega)$ of a dispersive fiber of length z as:

$$\underline{H}(z, j\Delta\omega) = \frac{\underline{A}(z, j\Delta\omega)}{\underline{A}(0, j\Delta\omega)} = \exp(-j\frac{\beta_2}{2}(\Delta\omega)^2 z) \tag{3.9}$$

so that the impulse response $h(z,t)$ of a fiber of length z is given by the inverse Fourier transform of 3.9.

Therefore, the dispersion compensating filter in frequency domain will be given by the inverse of the previous transfer function, i.e. the all-pass filter with transfer function $1/\underline{H}(z, j\Delta\omega)$. In the next section a time domain approximation to the design of the chromatic dispersion compensation filter is proposed.

3.2.2 Time domain design of the chromatic dispersion compensating filter

Taking the inverse Fourier transform of equation 3.9 and considering the relationship between β_2 and D from 2.14 we obtain the impulse response of the dispersive fiber that is given by:

$$h(z,t) = \sqrt{\frac{jc}{D\lambda^2 z}} \exp(-j\frac{\pi c}{D\lambda^2 z}t^2) \tag{3.10}$$

Hence, to calculate the output signal of the fiber for any random input, the convolution of the input signal with the impulse response will be calculated. The frequency domain transfer function of the chromatic dispersion compensation filter is written as:

$$H_{icd}(z, j(\omega)) = \exp(j\frac{\beta_2}{2}\omega^2 z) \tag{3.11}$$

Estimating the inverse Fourier transform from equation 3.11 we can state the time domain impulse response of the CD compensation filter $h_{icd}(z,t)$ as follows:

$$h_{icd}(z,t) = \sqrt{\frac{j}{2\pi\beta_2 z}} \exp(-j\frac{t^2}{2\beta_2 z}) \tag{3.12}$$

The implementation of the impulse response described by 3.12 has several drawbacks, such as it is non-causal and its duration is infinite. To be able to sample $h_{icd}(z,t)$, according to Nyquist-Shannon sampling theorem for avoiding aliasing effect, a band limited signal is required. Consequently, we have to truncate that impulse response yielding a finite duration response which will be able to be performed by a finite impulse response filter, whose diagram is shown in figure 3.3.
The FIR filters impulse response is described by:

$$h(n) = b_0\delta(n) + b_1\delta(n-1) + b_2\delta(n-2) + ... \tag{3.13}$$

Applying the Z-transform to equation 3.13 we obtain:

$$H(z) = b_0 + b_1 z^{-1} + b_2 z^{-2} + ... \tag{3.14}$$

Thus, by convolving the input signal $x(n)$ with the impulse response $h(n)$ of the FIR filter, the filter output signal $y(n)$ can be written as:

$$y(n) = b_0 x(n) + b_1 x(n-1) + ... + b_N x(n-N) \tag{3.15}$$

where b_i are the filter weights and N is the filter length. As a condition to find out the length of the truncation window, Nyquist frequency $f_s/2$ is applied. When taking into account that the frequency of the chirp increases with time as it is shown in equation 3.12, differentiating the phase of equation 3.12 with respect to time, the angular frequency can be written as:

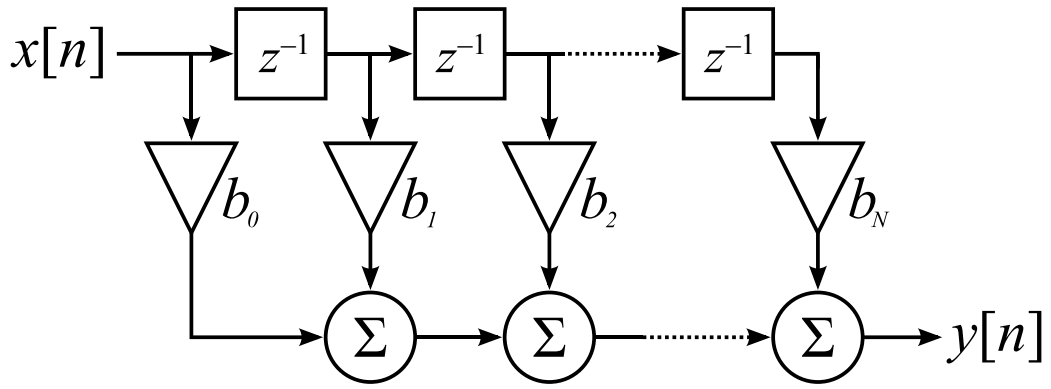

Figure 3.3: FIR filter diagram [22].

$$f = \frac{c}{D\lambda^2 z} t \tag{3.16}$$

where if $f = f_s/2$, we can find the value of t as:

$$t = \frac{D\lambda^2 z}{c}\frac{f_s}{2} = \frac{D\lambda^2 z}{2cT} \tag{3.17}$$

where T is the sampling period. So then the length of the truncation window will be expressed as next condition:

$$-\frac{D\lambda^2 z}{2cT} \leq t \leq \frac{D\lambda^2 z}{2cT} \tag{3.18}$$

As demonstrated by Savory in [4], the expression for the tap weights comes from equation 3.12 and it is stated as:

$$a_k = \sqrt{\frac{jcT^2}{D\lambda^2 z}} exp(j\frac{\pi cT^2}{D\lambda^2 z}k^2) \tag{3.19}$$

where, the number of taps is set to an odd number, considering the total number of taps as N:

$$-\left\lfloor \frac{N}{2} \right\rfloor \leq k \leq \left\lfloor \frac{N}{2} \right\rfloor$$

where $k = \frac{t}{T}$ has been applied to the criterion 3.18 yielding:

$$N = 2 \times \left\lfloor \frac{|D|\,\lambda^2 z}{2cT^2} \right\rfloor + 1$$

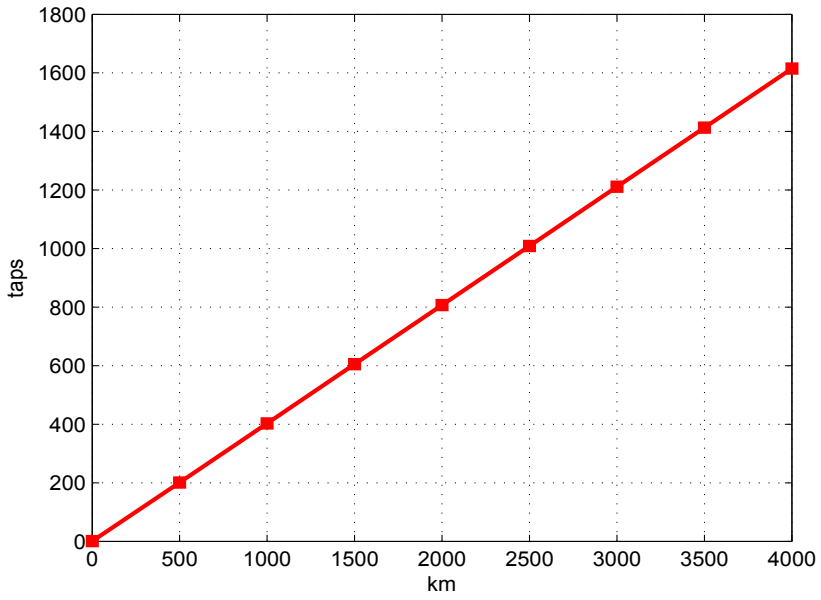

Figure 3.4: Number of taps required using Savory's method.

where N is the number of taps, T is the sampling period and $\lfloor x \rfloor$ is the integer part of x rounded towards minus infinity.
If we consider a large number of taps, then the sampled impulse response will approach the continuous time impulse response. According to this method, the number of taps is closely related to the fiber length z as shown in figure 3.4, the number of taps increases linearly with the propagation length. Furthermore, this is the upper bound of the number of taps N, with the resulting filter providing constant dispersion over the next frequency range:

$$-1/2T \leq f \leq 1/2T$$

3.3 Simulation results for chromatic dispersion compensation

In this section results of chromatic dispersion compensation performed in electrical domain using digital signal processing algorithms described in previous section are

presented. VPItransmissionMaker has been used as simulation tool to generate optical data analyzed in the next tests.

3.3.1 System setup

A 112 Gb/s dual polarization QPSK coherent optical transmission system constructed in *VPITransmissionMaker* is illustrated in figure 3.5. The simulation results reported were obtained for a 56 Gb/s single polarization QPSK coherent system, only one polarization from figure 3.5 was assessed.

The electrical data from two 28 Gb/s pseudo random bit sequence generators are sampled at twice the symbol-rate, this is used to provide the DSP interface with two samples/symbol data, which is filtered by a FIR filter for CD equalization (described in section 3.2) using MATLAB. The discretized signal obtained at the output of the FIR filter is then converted to the continuous domain by a Sample-and-Hold interpolator followed by low pass filtering. These two analog signals generated are the drive signals for the QPSK modulator. After passing through the modulator the optical signal is sent through a single-mode fiber. Finally, the coherent receiver converts the incoming signal into an electrical baseband signal by mixing it with an optical local oscillator (LO) and passing it through balanced photodetectors, then it is filtered by a low pass filter and sampled to get the In-phase and Quadrature signal waveforms.

A pseudo random bit sequence generated is used to provide the QPSK transmitter input. The generator is used to create a bit stream of 2^{16} bits, resulting in 2^{15} symbols since QPSK modulation is used. The laser wavelength used is 1550 nm, which corresponds to a carrier frequency of 193.1 THz. Since phase noise is not assessed in this section, the linewidth of the transmitted laser and the local oscillator laser are set to 0 Hz so that no phase noise is introduced. With regard to the optical fiber, parameters such as attenuation, nonlinear index and polarization mode dispersion (PMD) are set to 0 while the chromatic dispersion coefficient D is set to 16 ps/nm/km. In the coherent receiver, the 2x4 90 degree hybrid module is used to demodulate the received optical signal, which is composed of 3 dB 2x2 fiber couplers and a phase delay component of $\pi/2$ phase shift as it is depicted in figure 3.6. Additionally, as shown in figure 3.5, analogue to digital converters (ADC) are required. After low-pass filtering the recovered baseband signal is sampled at twice the symbol-rate to then be processed using MATLAB. In MATLAB the signal is filtered by a Normalized Least Mean Square (NLMS) filter in order to perform Nyquist noise filtering, removing any additive noise in the system. Finally, the symbol decisions are made and the bit error rate is assessed.

As it is illustrated in figure 3.7, using the NLMS filter in the receiver to remove any additive noise we obtain an improvement around 0.7 dB for a 10^{-3} BER for back-to-back propagation (without adding any fiber dispersion, setting fiber length equal to zero). Thus, it has been applied in all simulation results presented below. In this case, NLMS filter parameters such as the number of taps and step size were adjusted experimentally to achieve the best performance of the filter.

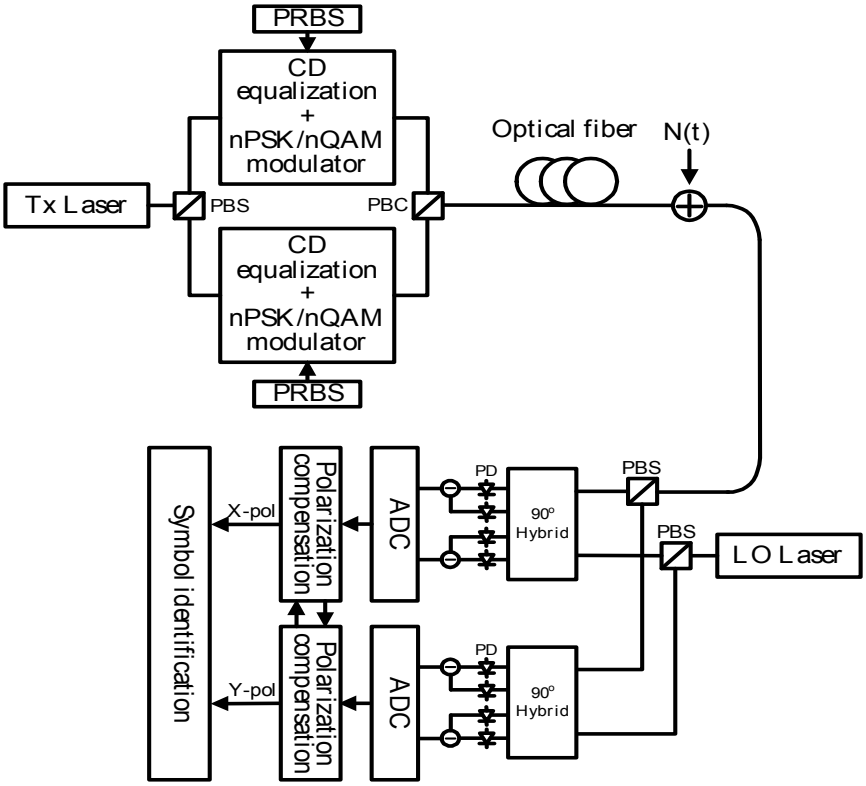

Figure 3.5: Schematic of 112 Gbit/s dual polarization nPSK/nQAM coherent transmission system using precompensation of chromatic dispersion. N(t) represents the added optical noise which is used to measure the bit error rate (BER) as a function of optical signal-to-noise ratio (OSNR). Figure abbreviations: Tx - transmitter; PBS - polarizing beam splitter; PBC - polarization beam combiner; PRBS - pseudo random bit sequence; LO - local oscillator; ADC - analogue to digital conversion; CD - chromatic dispersion.

In addition, the performance of the CD compensating FIR filter at the configuration with AM/PM modulators placed in cascade can be studied in figure 3.8, which shows bit-error-rate as a function of optical signal-to-noise ratio for back-to-back, 600km and 2000km transmission distances. It can be seen that the fiber chromatic dispersion is almost totally compensated by the linear FIR filter. The required OSNR penalty for 10^{-3} BER with respect to back-to-back operation is around 1.4 dB for both propagation distances of 600km and 2000km.

In relation to the DSP performance using the Cartesian Mach-Zehnder modulator as the electro-optic modulator, some results can be observed in figure 3.9.
In this case, from figure 3.9 it can be noticed about 1.4 dB optical signal-to-noise ratio penalty from back-to-back result at BER equal to 10^{-3} for both 600km and 2000km transmission distances.

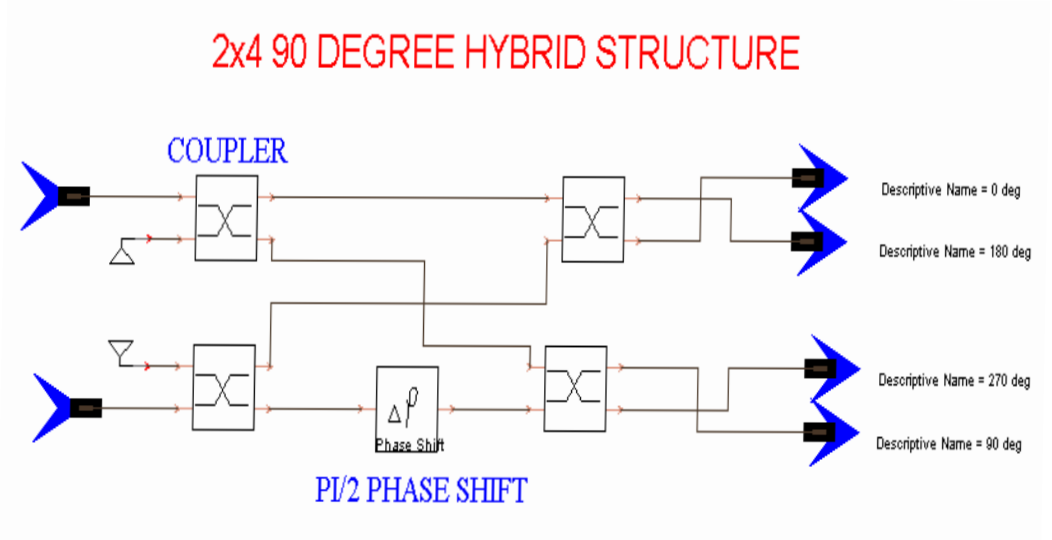

Figure 3.6: 90 Degree Hybrid Structure [17].

Therefore, Figures 3.8 and 3.9 show that at 600 km and 2000 km filter lengths of 243 and 807 taps respectively are needed to mitigate chromatic dispersion effects. It is also important to note that for different transmission distances, increasing the number of taps of the FIR filter does not increase the OSNR penalty required which remains nearly constant. It has been shown that for a 10^{-3} BER the OSNR penalty required is around 1.4 dB with respect to back-to-back value for any fiber length. Hence the chromatic dispersion is almost fully compensated by the linear FIR filter. The penalty achieved respecting back-to-back operation using either ideal AM/PM serial configuration or Cartesian Mach-Zehnder modulator is believed to be due to many factors, for example the signal conversion carried out by the digital to analog converter at the transmitter and also by the analog-to-digital converter at the receiver. It may also be caused by the continuous to discrete conversion of the FIR impulse response which increases the penalty obtained. The fact that we have to remove some samples from the beginning of the convolved signal before doing the bit error rate calculation may also decreases the system performance.

Furthermore, a comparison between using an AM/PM serial configuration or a Cartesian MZM as the optical modulator is illustrated in figure 3.10.
As expected, from figure 3.10, which shows BER against OSNR plot for back-to-back operation, it can be noticed that the Cartesian Mach-Zehnder modulator due to its non-ideal structure works with about 0.5 dB penalty at 10^{-3} BER compared to the performance of the ideal AM/PM serial modulator.

Additionally, it is important to comment that, as it was accurately shown in [3], the FIR filter used for fiber chromatic dispersion compensation in the receiver for a post-compensation system described by Savory's algorithm [4] does not entirely

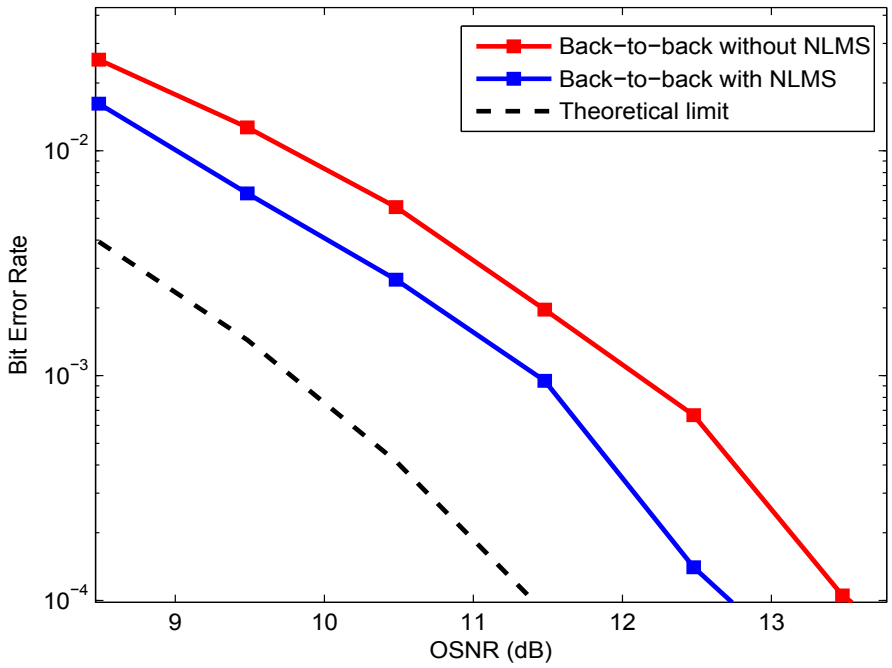

Figure 3.7: BER vs. OSNR in a QPSK system, comparison for back to back configuration with/without using NLMS filtering in the receiver.

compensate the CD for short fibers, specifically fiber lengths below 300 km. On the same way, it has been shown that for the pre-compensation scheme implemented in this thesis, the same behavior for the FIR filter was achieved.

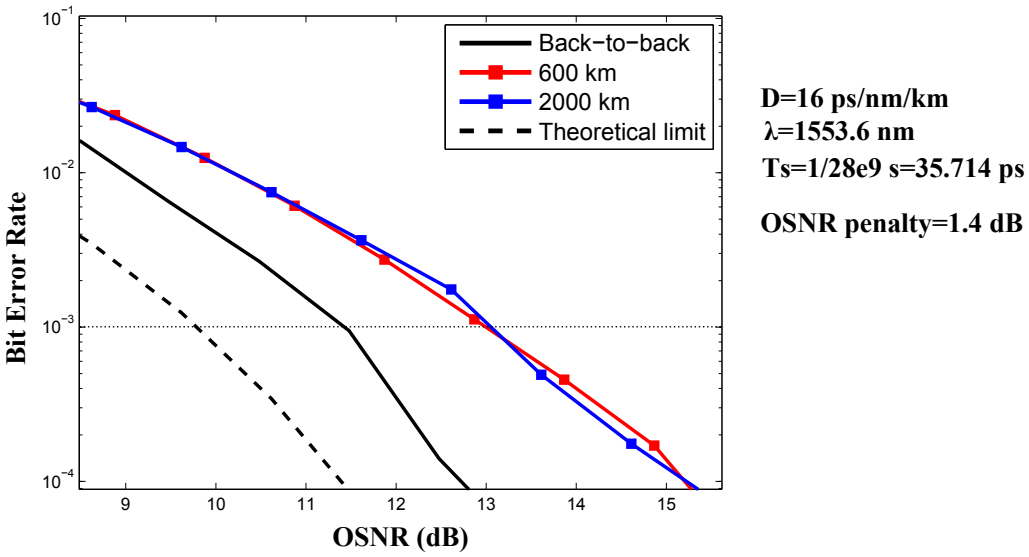

Figure 3.8: BER vs. OSNR in a single polarization QPSK coherent system using modulator in serial configuration for linear precompensation of chromatic dispersion. Results are for different propagation distances, for back-to-back, 600km (243 taps), 2000km (807 taps) indicated in the figure. The PRBS length is $2^{16} - 1$. Figure abbreviations: OSNR- Optical Signal-to-Noise Ratio.

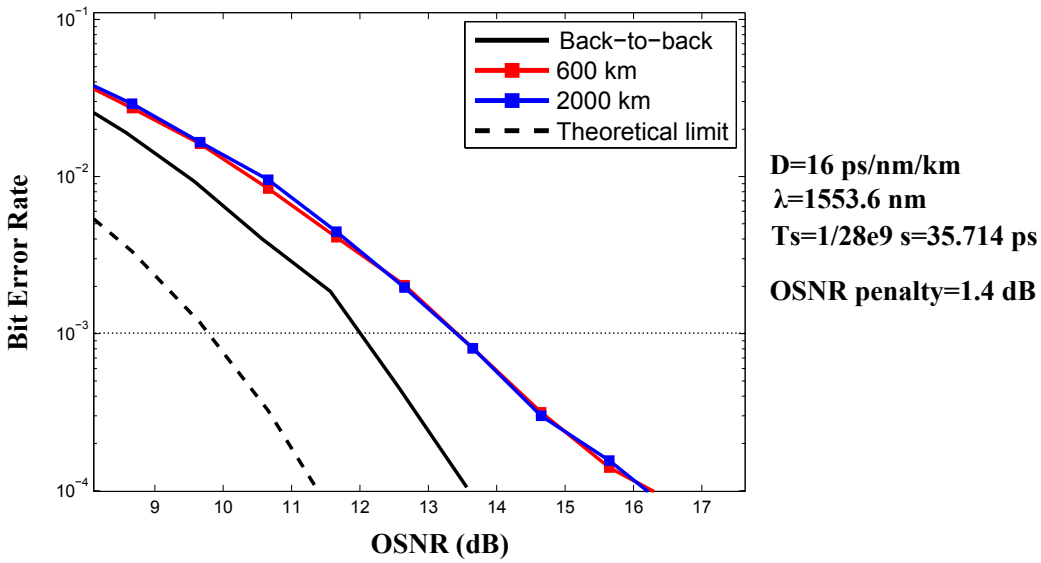

Figure 3.9: BER vs. OSNR for single polarization QPSK coherent system using Cartesian Mach-Zehnder modulator for linear precompensation of chromatic dispersion. Results are for different propagation distances for back-to-back, 600km (243 taps), 2000km (807 taps) indicated in the figure. The PRBS length is $2^{16} - 1$. Figure abbreviations: OSNR-Optical Signal-to-Noise Ratio.

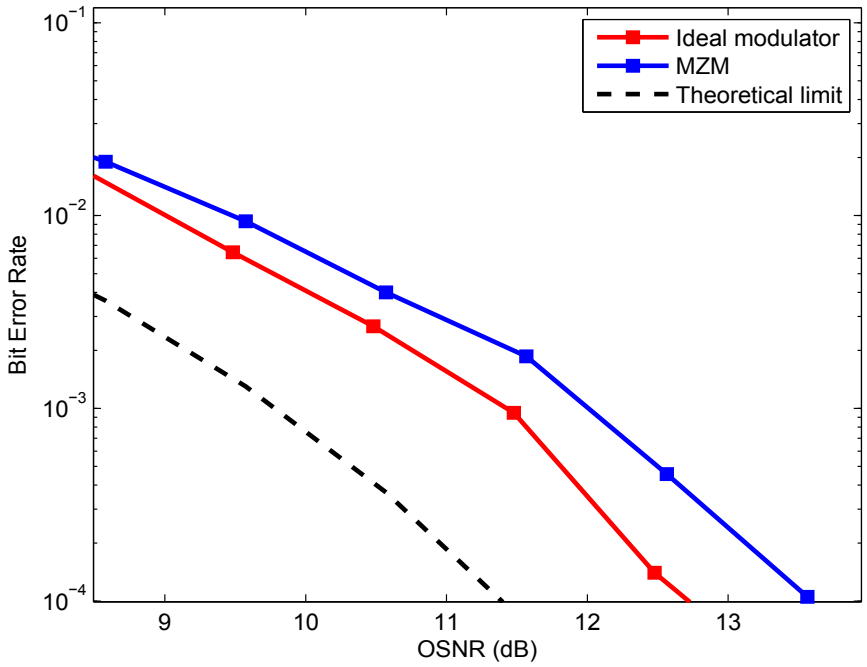

Figure 3.10: Comparison between ideal AM/PM serial and Cartesian MZM configurations for back to back propagation.

Chapter 4

Phase Noise Compensation

Semiconductor lasers introduce two types of noise: *intensity noise*, i.e. variations in the optical power level of a laser, and *phase noise*, i.e. random fluctuations of the frequency in the time domain of the laser output signal.

Ideally, the spectrum of the laser output signal is a delta function centered at the laser's frequency ω_0, i.e. all the signal's power is at a single frequency. However, in reality the signal power is spread out to adjacent frequencies, as can be seen in figure 4.1, resulting in noise sidebands. This undesirable power distribution centered around the laser frequency is the phase noise effect.

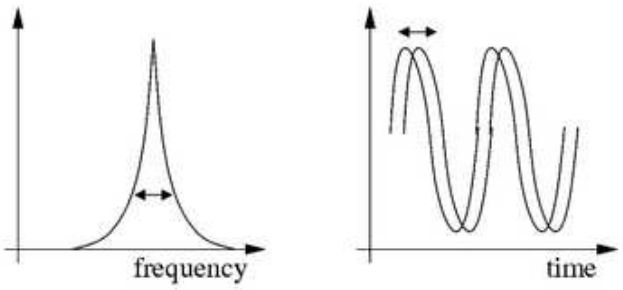

Figure 4.1: Phase noise effect in time and frequency domain.

Considering the following noise free output signal of the laser [16]:

$$E_{out}(t) = \sqrt{P(t)}\exp(j\omega_0 t)$$

Phase noise is added to this signal by adding a stochastic process represented by $\varphi(t)$ as follows:

$$E_{out}(t) = \sqrt{P(t)}\exp(j\omega_0 t + \varphi(t))$$

where $P(t)$ and $\varphi(t)$ are time-varying functions and ω_0 is the laser fundamental frequency.

To compensate phase noise efficiently carrier recovery systems are widely deployed estimating the phase differences between a received signal's carrier and the receiver's local oscillator in order to carry out the coherent demodulation.

Carrier phase estimation can be accomplished by using Phase-Locked Loop (PLL). PLL's have been fairly commonly used in digital communications receivers to remove any frequency/phase offsets that might exist between the transmitter and receiver oscillators. However, the use of digital signal processing algorithms with feed-forward and feed-back architectures for carrier phase estimation is becoming an interesting alternative due to its effectiveness in decreasing phase noise fluctuations from laser sources [23].

4.1 LMS filtering for carrier phase estimation

Many DSP algorithms implemented for carrier phase recovery are based on adaptive filtering. Adaptive filters are sometimes required because the filtering needs to be time-varying. These filters are characterized by their tap weights being adjusted automatically according to an specific optimization algorithm which is controlled by an error signal which is the difference between the reference signal and the estimated signal produced by the adaptive filter. The filters aim is not to totally cancel the error signal, but to minimize the error signal power. The general setup of an adaptive filter is shown in figure 4.2,

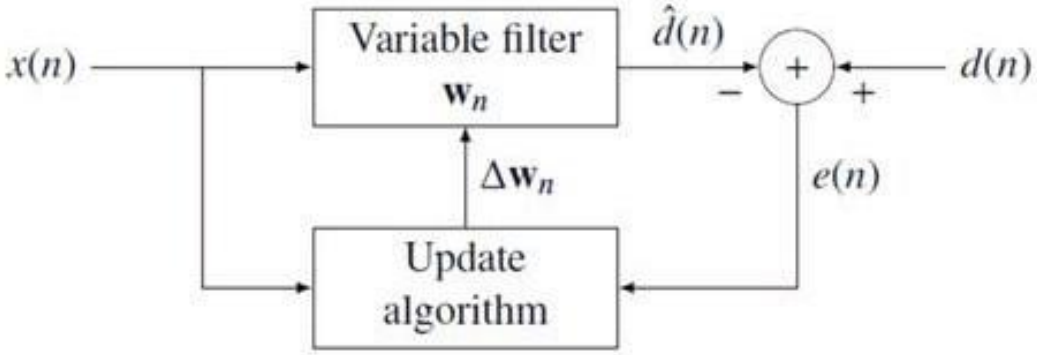

Figure 4.2: Block Diagram of an Adaptive Filter.

The *Variable filter* has a Finite Impulse Response (FIR) structure [22].
$x(n)$ is the input signal, $w(n)$ are the filter tap weights, $d(n)$ represents the desired signal, $\widehat{d}(n) = x(n) * w(n) = \sum_{k=0}^{L} (w_k(n) \cdot x(n-k))$ is the filter output, $e(n) = d(n) - \widehat{d}(n)$ is the error signal, and $w(n+1) = w(n) + \Delta w(n)$ is the updating equation, $\Delta w(n)$ is a correction factor for the filter coefficients.

The different algorithms used to update the tap weights defines a different correction factor according to the input and error signals. One algorithm that can be used to update the tap weights is Least Mean Squares (LMS), the performance of which is studied in this thesis.

4.1.1 Principle of normalized Least Mean Square filter

In a Least Mean Square filter implementation the tap weights are calculated in order to produce the least mean squares of the error signal, based on the gradient algorithm [22].
Using vectorial notation:

$$\underline{w}_{n+1} = \underline{w}_n - \mu\hat{\underline{\nabla}}\epsilon(\underline{w}_n)$$

where

$$\hat{\underline{\nabla}}\epsilon = -2e(n) \cdot \underline{X}(n)$$

Assuming the process starts at instant n with two samples: $x(n)$ and $d(n)$, the algorithm steps are:

1. Updating $\underline{X}$ with the new $x(n)$.
2. Calculating the sample $y(n)$ by filtering $x(n)$: $y(n) = \underline{W}_n{}^T \cdot \underline{X}$.
3. $e(n)$ estimation: $e(n) = d(n) - y(n)$.
4. Updating $\underline{\mathrm{W}}$ for the instant $n + 1$:

$$\underline{W}_{n+1} = \underline{W}_n + 2\mu \cdot e(n) \cdot \underline{X}(n)$$

At time n the tap weights are calculated for time $n + 1$ (before it starts) by using information from previous instant n.

The parameter μ is the step size, a critical parameter in adaptive filters since it is closely related to the convergence speed of the algorithm. If μ is set at a low value, the convergence will be slow and high precision will be obtained, whereas high μ values lead to a faster convergence, but lower precision.

Additionally, a one-tap normalized LMS filter (NLMS) is a variant of the LMS algorithm that normalizes the signal by the input signal power ensuring the stability of the algorithm, will be used in this thesis for carrier phase estimation.
Its updating equation is expressed as [24]:

$$w_{NLMS}(n+1) = w_{NLMS}(n) + \frac{\mu_{NLMS}}{|x_{PN}(n)|^2} x^*_{PN}(n) e_{NLMS}(n)$$

with

$$e_{NLMS}(n) = d_{PE}(n) - w_{NLMS}(n) \cdot x_{PN}(n)$$

where $w_{NLMS}(n)$ is the complex tap weight, $x_{PN}(n)$ is the complex magnitude of the input signal, n represents the number of the symbol sequence, $d_{PE}(n)$ is the desired symbol, $e_{NLMS}(n)$ is the estimation error between the desired symbols and the filter output signal, and μ_{NLMS} is the step size coefficient.

4.2 Phase noise influence in coherent transmission systems with digital chromatic dispersion equalization

This section introduces a comparative study of the equalization enhanced phase noise (EEPN) for pre- and post-compensation of chromatic dispersion in high speed transmission systems.

In coherent optical systems many of the algorithms previously mentioned are used for carrier phase extraction. Those algorithms usually assess the phase noise in the transmitter and local oscillator lasers, regardless of the chromatic dispersion effect on the phase noise in the system. Hence here it will be studied the interaction between the digital chromatic dispersion equalization and the laser phase noise due to equalization enhanced phase noise when the dispersion compensation is performed either at the transmitter (pre-compensation) or at the receiver (post-compensation) [25].

4.2.1 EEPN influence in post-compensation system

The design of a coherent optical communication system with digital chromatic dispersion equalization at the receiver and carrier phase estimation is illustrated in figure 4.3 [24].

When the phase noise is only added by the transmitter laser, it passes through the optical fiber and the CD equalization module, hence the dispersion associated to the transmitter laser phase noise is approximately zero (the additional noise due to the EEPN effect will be zero). However, when the phase noise is introduced by the local oscillator (LO) laser at the receiver, it only goes through the CD equalization module leading to dispersion in the transmission system resulting in a significant equalization enhanced phase noise (EEPN).

Theoretical studies demonstrate that for post-compensation systems the variance of the noise due to the EEPN is linearly proportional to the chromatic dispersion and the linewidth of the LO laser, as shown in the expression 4.1 [24]:

$$\sigma^2_{EEPN} = \frac{\pi\lambda^2}{2c} \cdot \frac{D \cdot L \cdot \Delta f_{LO}}{T_s} \equiv 2\pi\Delta f_{EE} \cdot T_s \tag{4.1}$$

where λ is the central wavelength of the transmitted optical carrier wave, c is the speed of light in vacuum, D is the chromatic dispersion coefficient of the optical fiber, L is the fiber length, Δf_{LO} is the 3-dB linewidth of the LO laser and T_s is the symbol period of the transmission system.

As mentioned previously a one-tap NLMS filter is used to compensate for the phase noise effect. It is important to note that the step size in the NLMS filter was optimized empirically to give the best performance of the filter for a certain laser phase noise.

The BER floor of phase estimation using NLMS filtering with equalization

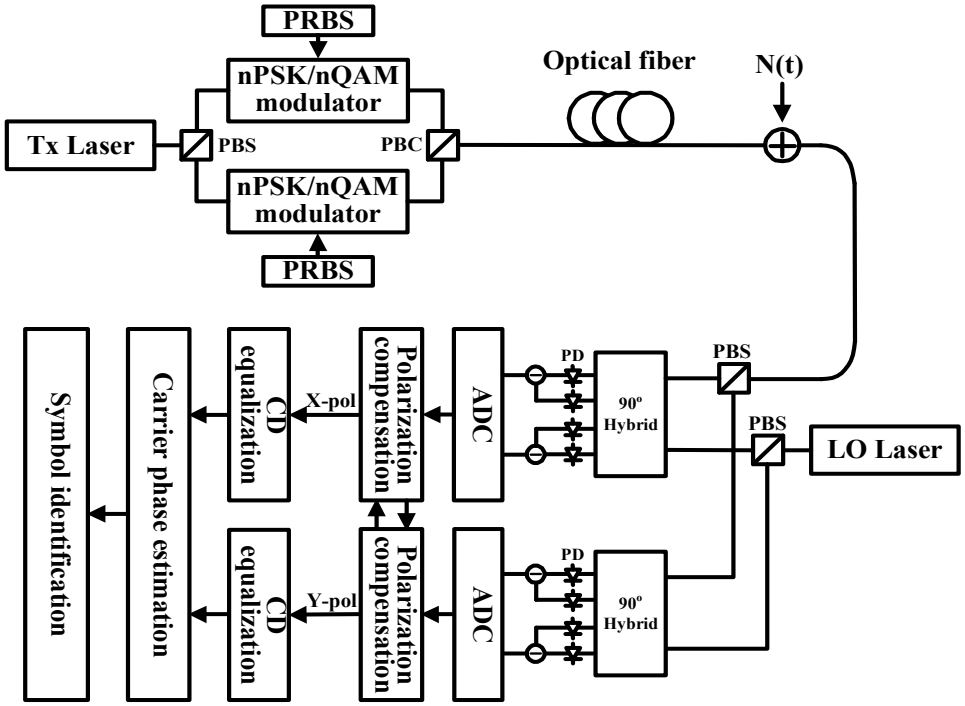

Figure 4.3: Block diagram for dual polarization nPSK/nQAM system using post-compensation of chromatic dispersion influence. N(t) represents the added optical noise which is used to measure the bit error rate (BER) as a function of optical signal-to-noise ratio (OSNR). Figure abbreviations: Tx - transmitter; PBS - polarizing beam splitter; PBC - polarization beam combiner; PRBS - pseudo random bit sequence; LO - local oscillator; ADC - analogue to digital conversion; CD - chromatic dispersion.

enhanced phase noise has the analytical expression described by [24]:

$$BER_{floor}^{NLMS} \approx \frac{1}{2} \cdot erfc\left(\frac{\pi}{4\sqrt{2\sigma}}\right) \tag{4.2}$$

erfc designates the complementary error function.

$$\sigma^2 \approx \sigma_{TX}^2 + \sigma_{LO}^2 + \sigma_{EEPN}^2 \tag{4.3}$$

$$\sigma_{TX}^2 = 2\pi\Delta f_{TX} \cdot T_s \tag{4.4}$$

$$\sigma_{LO}^2 = 2\pi\Delta f_{LO} \cdot T_s \tag{4.5}$$

where σ^2 is the total phase noise variance in the coherent transmission system, σ^2_{TX} and σ^2_{LO} are the original phase noise variance of the transmitter (TX) and the local oscillator lasers respectively, Δf_{TX} is the 3-dB linewidth of the transmitter laser and Δf_{LO} is the 3-dB linewidth of the local oscillator. It is assumed that σ^2_{TX}, σ^2_{LO} and σ^2_{EEPN} are statistically independent.

In terms of effective linewidth, we can describe the total phase noise in the coherent system influenced by EEPN as follows:

$$\Delta f_{Eff} = \frac{\sigma^2_{TX} + \sigma^2_{LO} + \sigma^2_{EEPN}}{2\pi T_s} \approx \frac{\sigma^2}{2\pi T_s} \tag{4.6}$$

4.2.2 EEPN influence in pre-compensation system

For pre-compensation systems (shown in figure 4.4) the phase noise introduced by the local oscillator laser is not influenced by the chromatic dispersion effect since the chromatic dispersion of the optical fiber has been compensated by the CD equalization module in the transmitter. Hence in this case the EEPN effect can be ignored.
On the other hand, the phase noise added by the transmitter laser passes through the optical fiber getting distorted by the fiber chromatic dispersion. In this case the dispersion of the CD equalization filter does not interact with the transmitter laser phase noise. That means that for the pre-compensation setup the EEPN will be linearly proportional to the chromatic dispersion coefficient of the fiber D and the Δf_{TX} instead of the Δf_{LO} as shown in the formula 4.1.

4.2.3 Simulation results of the influence of CD compensation on EEPN in coherent systems

In this section simulation results for 56 Gbit/s QPSK coherent systems (28 GSymb/s) are presented. Only a single polarization from the system described in the figure 4.4 is used. Both impairments in coherent transmission systems, chromatic dispersion and phase noise, are treated separately by different modules.

For chromatic dispersion equalization a finite impulse response filter is implemented, in the same way as described in section 3.2, in which the number of taps depends on the length of the transmission fiber. The optical fiber used is a single mode fiber with a dispersion coefficient $D = 16\ pseg/nm/km$, two samples per symbol period is assumed. Besides, as explained above, a NLMS filter is used for phase noise compensation where an optimized step size is used on a case per case basis. The phase noise introduced by the transmission and local oscillator lasers are configured with a Gaussian probability density function. All the simulations have been performed in the VirtualPhotonics system simulation software environment [26].
Figure 4.5 shows the bit-error-rate versus optical signal-to-noise-ratio for a 2000 km transmission distance in the post-compensation system. For a value of the local oscillator laser linewidth Δf_{LO} of 5 MHz we get an EEPN linewidth Δf_{EE} of 206

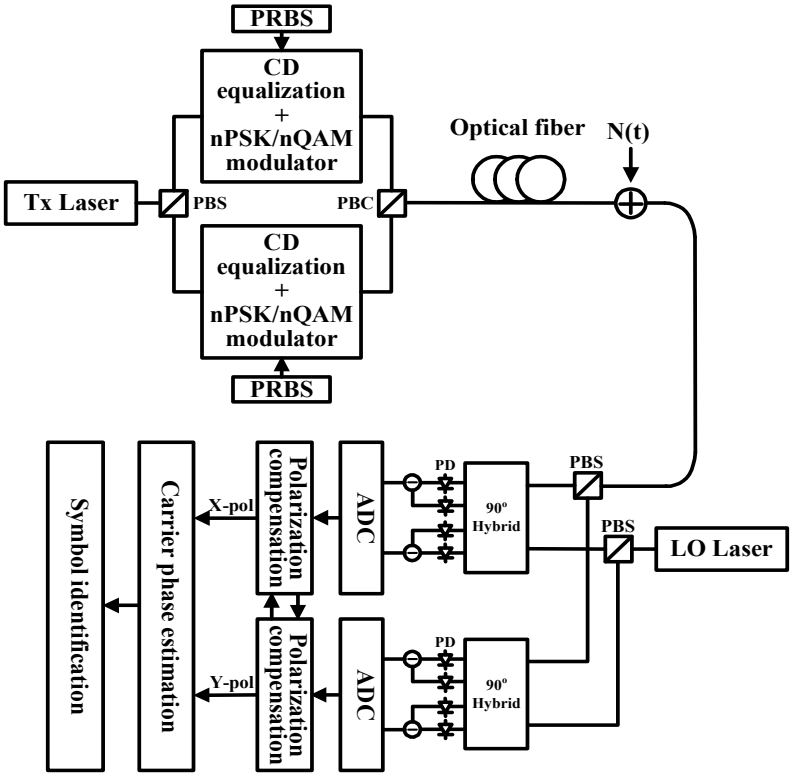

Figure 4.4: Block diagram for dual polarization nPSK/nQAM system using pre-compensation of chromatic dispersion influence. N(t) shows the added optical noise which is used to measure the bit error rate (BER) as a function of optical signal-to-noise ratio (OSNR). Figure abbreviations: Tx - transmitter; PBS - polarizing beam splitter; PBC - polarization beam combiner; PRBS - pseudo random bit sequence; LO- local oscillator; ADC - analogue to digital conversion; CD - chromatic dispersion.

MHz from eq. 4.1. For $\Delta f_{LO} = 10$ MHz the EEPN linewidth is 412 MHz. BER results for a total laser linewidth ($\Delta f_{TX} + \Delta f_{LO}$) of 10 MHz were obtained for next three different conditions:

1. $\Delta f_{TX} = 10$ MHz, $\Delta f_{LO} = 0$
2. $\Delta f_{TX} = \Delta f_{LO} = 5$ MHz
3. $\Delta f_{LO} = 10$ MHz, $\Delta f_{TX} = 0$

From the figure 4.5 it can be seen that when the local oscillator laser linewidth is zero, which means we have no EEPN influence, the BER-floor is below 10^{-3}. For a

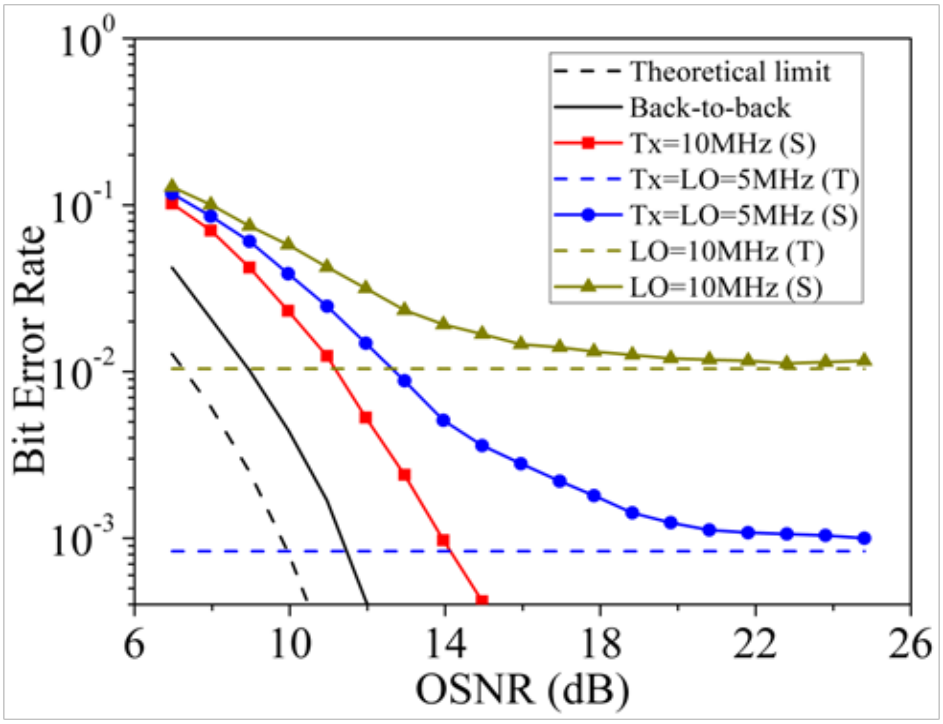

Figure 4.5: BER for single polarization QPSK coherent system using post-compensation of chromatic dispersion. Results are for a transmission distance of 2000 km. Different cases are indicated in the figure. Tx and LO laser linewidths are indicated in the figure. The PRBS length is $2^{16} - 1$. Figure abbreviations: OSNR - optical signal-to-noise ratio; Rx - receiver; RF - radio frequency; S - simulation results; T - BER floor using theoretical expression.

local oscillator linewidth of 10 MHz we have the largest EEPN influence causing the BER-floor to reach circa 10^{-2} and we have notable agreement with the prediction of 4.2. With a linewidth of 5 MHz for both lasers results in a BER floor of around 10^{-3} in accordance with the theoretical expression in 4.2.
Moreover, in figure 4.6 the BER versus OSNR results for the pre-compensation system implementation can be seen, for the same three cases as for the post-compensation system considered in figure 4.5.

Comparing the two figures from post- and pre- compensation configurations, it is important to say that for the pre-compensation case the most relevant contribution of EEPN is caused when the phase noise is introduced by the transmitter laser. It is also important to note that a marginally poorer agreement between the BER-floor predicted analytically by 4.2 and the simulation results for the pre-compensation

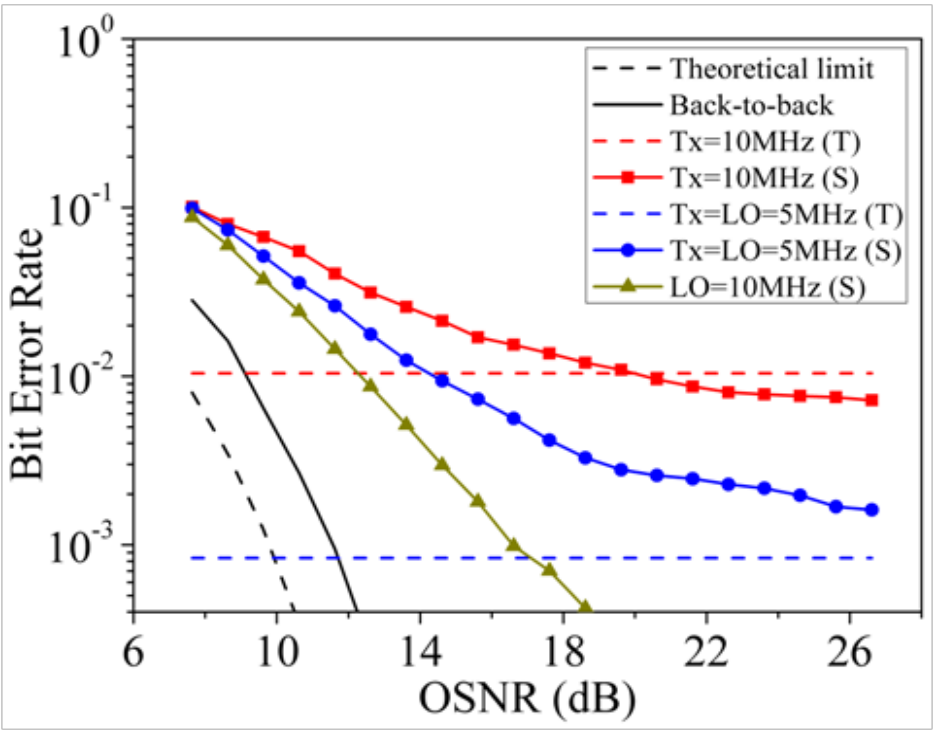

Figure 4.6: BER for single polarization QPSK coherent system using pre-compensation of chromatic dispersion. Results are for a transmission distance of 2000 km. The different cases are indicated in the figure, as well as transmission and local oscillator laser linewidths. The PRBS bit sequence length is $2^16 - 1$. Figure abbreviations: OSNR - optical signal-to-noise ratio; Rx - receiver; RF - radio frequency; S - simulation results; T - BER floor using the theoretical expression.

case is achieved. Experimentally this issue may be related to the fact that different optimum step size is used in the NLMS filtering for carrier phase estimation in the pre- and post-compensation systems [24].

These results achieved by implementing chromatic dispersion equalization in the electrical domain could be improved by performing CD compensation in optical domain. It has been shown that using dispersion compensating fibers, where the CD is compensated in optical domain, the EEPN effect may be neglected getting a much lower BER [25].

Chapter 5

Conclusions and future work

5.1 Conclusions

Most research in coherent optical communications have been focused on compensating fiber impairments at the receiver. In this thesis a 56 Gb/s QPSK coherent optical transmission system based on digital electronic predistortion has been studied with the goal of mitigating the linear impairments of an optical fiber.

Electronic predistortion was implemented with digital signal processing implementing a linear finite impulse response filter placed in the transmitter in order to compensate for chromatic dispersion in the electrical domain by generating predistorted signals.

At the transmitter different electro-optical modulators have been assessed, first an ideal amplitude/phase modulators placed in cascade and then a Cartesian Mach-Zehnder modulator.

For both configurations, results have shown that using a predistorting FIR filter at the transmitter, whose largest number of taps was set according to the maximum truncation window limited by the Nyquist criterion, can compensate a large amount of chromatic dispersion by reversing the fiber chromatic dispersion effect. However, there are some factors that decrease the system performance, e.g. conversion between the analog and digital domain performed by the ADCs and DACs at the receiver and transmitter respectively, besides digitizing the continuous impulse response of the optical fiber also contributes to limit the system performance increasing the OSNR required for a certain BER value. Another limitation of the FIR filter approach is that it is not possible to mitigate the nonlinear impairments caused by the optical fiber. That constraint could be solved by using programmable look-up tables (LUT) instead of a FIR filter.

The impact of dispersion equalization enhanced phase noise (EEPN) has been evaluated for both pre- and post-compensation of chromatic dispersion in coherent transmission systems. In both cases, chromatic dispersion equalization has been accomplished through linear FIR filtering, whereas a one-tap normalized LMS filter was implemented for carrier phase estimation. Comparing the results for both

configurations, it can be concluded that for postcompensation setup, the EEPN influence is limited by the local oscillator laser phase noise, while in precompensation systems the transmitter laser is the main source of EEPN in the transmission system. These constraints can be solved by compensating fiber chromatic dispersion in optical domain using dispersion compensation fibers in such a way that the EEPN impact could be neglected.

5.2 Future Work

As for future work it would be intriguing to analyze different DSP algorithms that can be used at the transmitter to electronically compensate for nonlinear impairments in the optical fiber for dual-polarization precompensation schemes, in order to not only mitigate chromatic dispersion but also some nonlinear effects such as self-phase modulation. It would be also interesting to investigate the behavior of precompensation systems, performing the equalization of fiber chromatic dispersion also in electrical domain, but studying the impact of equalization enhanced phase noise in the system adding the transmitter laser phase noise in electrical domain. In that way it could be possible to reduce the dispersion caused by the transmitter phase noise to almost zero.

References

[1] Govind P. Agrawal. *Fiber-optic Communication Systems 3rd Edition.* Willey, 2002.

[2] Peter J. Winzer and René-Jean Essiambre. Advanced Optical Modulation Formats. *Proceedings of the IEEE, Vol. 94, No. 5*, 2006.

[3] Tianhua Xu, Gunnar Jacobsen, Sergei Popov, Jie Li, Evgeny Vanin, Ke Wang, Ari T. Friberg, and Yimo Zhang. Chromatic dispersion compensation in coherent transmission system using digital filters. *Optics Express 16243, Vol. 18, No. 15*, 2010.

[4] Seb J. Savory. Digital filters for coherent optical receivers. *Optics Express 804, Vol. 16, No. 2*, 2008.

[5] Jens C. Rasmussen, Takeshi Hoshida, and Hisao Nakashima. Digital Coherent Receiver Technology for 100-Gb/s Optical Transport Systems. *Fujitsu Sci. Tech. J., Vol. 46, No. 1, pp. 63-71*, 2010.

[6] Robert Killey, Philip Watts, Vitaly Mikhailov, Madeleine Glick, and Polina Bayvel. Electronic dispersion compensation by signal predistortion using a dual-drive Mach-Zehnder modulator. *IEEE Photonics Technology letters, Vol. 17, No. 3*, 2005.

[7] J. McNicol, M. O'Sullivan, K. Roberts, A. Comeau, D. McGhan, and L. Strawczynski. Electrical Domain Compensation of Optical Dispersion. *Submitted for publication in Optical Fiber Communications*, 2004.

[8] Robert Waegemans, Stefan Herbst, Ludwig Holbein, Philip Watts, Polina Bayvel, Cornelius Fürst, and Robert Killey. 10.7 Gb/s electronic predistortion transmitter using commercial FPGAs and D/A converters implementing real-time DSP for chromatic dispersion and SPM compensation. *Optics Express 8630, Vol. 17, No. 10*, 2009.

[9] Philip Watts, Polina Bayvel, Robert Killey, and Madeleine Glick. Electronic dispersion compensation by signal predistortion. *Submitted for publication in Optical Communications*, 2006.

[10] Liang Dou, Zhenning Tao, Lei Li, Weizhen Yan, Takahito Tanimura, Takeshi Hoshida, and Jens C. Rasmussen. A Low Complexity Pre- Distortion Method for Intra-channel Nonlinearity. *Submitted for publication in Optical Fiber Communications*, 2011.

[11] Christian Weber, Johannes K. Fisher, Christian Bunge, and Klaus Petermann. Electronic precompensation of intrachannel nonlinearities at 40 Gb/s. *IEEE Photonics Technology Letters, Vol. 18, No. 16, pp. 1759-1761*, 2006.

[12] Philip Watts, Robert Waegemans, Madeleine Glick, Polina Bayvel, and Robert Killey. An FPGA-Based Optical Transmitter Design Using Real-Time DSP for Advanced Signal Formats and Electronic Predistortion. *Journal of Lightwave Technology, Vol. 25, No. 10*, 2007.

[13] Philip Watts, Robert Waegemans, Yannis Benlachtar, Vitaly Mikhailov, Polina Bayvel, and Robert Killey. 10.7 Gb/s transmission over 1200 km of standard single-mode fiber by electronic predistortion using FPGA-based real-time digital signal processing. *Optics Express 12171, Vol. 16, No. 16*, 2008.

[14] Keang-Po Ho and Joseph M. Kahn. Spectrum of Externally Modulated Optical Signals. *Journal of Lightwave Technology, Vol. 22, No. 2*, 2004.

[15] Shaham Sharifian. Chromatic dispersion compensation by signal predistortion: Linear and nonlinear filtering. Master's thesis, Chalmers University of Technology, Goteborg, Sweden, 2010.

[16] Jose Company, Francisco J. Fraile Peláez, and Javier Marti. *Fundamentos de Comunicaciones Opticas*. Ed. Síntesis, Madrid, ISBN 84-7738-599-8, 1998.

[17] Marco Mussolin. DSP Algorithms for High-Speed Coherent Transmission in Optical Fibers. Master's thesis, KTH-ICT/MAP/Optics, 2010.

[18] John G. Proakis. *Communication Systems Engineering*. Ed. Prentice Hall, 1994.

[19] J. J. Lepley, J. G. Ellison, S. G. Edirisinghe, A. S. Siddiqui, and S. D. Walker. Excess penalty impairments of polarization shift keying transmission format in presence of polarization mode dispersion. *Electron. Lett., Vol. 36, No. 8, pp. 736-737*, 2000.

[20] Dirk van den Borne, Vincent A. J. M. Sleiffer, Mohammad S. Alfiad, Sander L. Jansen, and Torsten Wuth. POLMUX-QPSK mdulation and coherent detection: the challenge of long-haul 100 G transmission. *ECOC*, 2009.

[21] Seb J. Savory, Giancarlo Gavioli, Robert Killey, and Polina Bayvel. Electronic compensation of chromatic dispersion using a digital coherent receiver. *Optics Express 2120, Vol. 15, No. 5*, 2007.

[22] Antonio Albiol, Valery Naranjo, and Josep Prades. *Tratamiento Digital de la Señal. Teoría y Aplicaciones*. SPUPV-99.4162, 2007.

[23] Tianhua Xu. *Digital Dispersion Equalization and Carrier Phase Estimation in 112 Gbit/s Coherent Optical Fiber Transmission System.* PhD thesis, Royal Institute of Technology (KTH), 2011.

[24] Tianhua Xu, Gunnar Jacobsen, Sergei Popov, Jie Li, Ari T. Friberg, and Yimo Zhang. Analytical estimation of phase noise influence in coherent transmission system with digital dispersion equalization. *Optics Express 7756, Vol. 19, No. 8*, 2011.

[25] Gunnar Jacobsen, Marisol Lidon, Tianhua Xu, Sergei Popov, Ari T. Friberg, and Yimo Zhang. Influence of pre- and post-compensation of CD on EEPN in coherent multilevel systems. *Submitted for publication in Journal of Optical Communications*, 2011.

[26] www.vpiphotonics.com.